Received: 17 March 2021 | Revised: 2 July 2021 | Accepted: 13 July 2021

DOI: 10.1002/psc.3362

SPECIAL ISSUE REVIEW

Journal of PeptideScience WILEY

Self-assembling systems comprising intrinsically disordered protein polymers like elastin-like recombinamers

Diana Juanes-Gusano | Mercedes Santos | Virginia Reboto | Matilde Alonso | José Carlos Rodríguez-Cabello

BIOFORGE (Group for Advanced Materials and Nanobiotechnology) CIBER-BBN, Edificio Lucía, University of Valladolid, Valladolid, Spain

Correspondence
José Carlos Rodríguez-Cabello, BIOFORGE (Group for Advanced Materials and Nanobiotechnology), CIBER-BBN, Edificio Lucía, University of Valladolid, Paseo de Belén 19, Valladolid 47011, Spain.
Email: roca@bioforge.uva.es

Funding information
Centro en Red de Medicina Regenerativa y Terapia Celular de Castilla y León; Interreg V España Portugal POCTEP, Grant/Award Number: 0624_2IQBIONEURO_6_E; Junta de Castilla y León, Grant/Award Numbers: VA317P18, Infrared2018-UVA06; Spanish Government, Grant/Award Numbers: PID2019-110709RB-100, RED2018-102417-T, RTI2018-096320-B-C22, MAT2016-78903-R

Despite lacking cooperatively folded structures under native conditions, numerous intrinsically disordered proteins (IDPs) nevertheless have great functional importance. These IDPs are hybrids containing both ordered and intrinsically disordered protein regions (IDPRs), the structure of which is highly flexible in this unfolded state. The conformational flexibility of these disordered systems favors transitions between disordered and ordered states triggered by intrinsic and extrinsic factors, folding into different dynamic molecular assemblies to enable proper protein functions. Indeed, prokaryotic enzymes present less disorder than eukaryotic enzymes, thus showing that this disorder is related to functional and structural complexity. Protein-based polymers that mimic these IDPs include the so-called elastin-like polypeptides (ELPs), which are inspired by the composition of natural elastin. Elastin-like recombinamers (ELRs) are ELPs produced using recombinant techniques and which can therefore be tailored for a specific application. One of the most widely used and studied characteristic structures in this field is the pentapeptide $(VPGXG)_n$. The structural disorder in ELRs probably arises due to the high content of proline and glycine in the ELR backbone, because both these amino acids help to keep the polypeptide structure of elastomers disordered and hydrated. Moreover, the recombinant nature of these systems means that different sequences can be designed, including bioactive domains, to obtain specific structures for each application. Some of these structures, along with their applications as IDPs that self-assemble into functional vesicles or micelles from diblock copolymer ELRs, will be studied in the following sections. The incorporation of additional order- and disorder-promoting peptide/protein domains, such as α-helical coils or β-strands, in the ELR sequence, and their influence on self-assembly, will also be reviewed. In addition, chemically cross-linked systems with controllable order–disorder balance, and their role in biomineralization, will be discussed. Finally, we will review different multivalent IDPs-based coatings and films for different biomedical applications, such as spatially controlled cell adhesion, osseointegration, or biomaterial-associated infection (BAI).

KEYWORDS
biomineralization, elastin-like recombinamers (ELRs), intrinsically disordered proteins (IDPs), order–disorder, protein domains, self-assembly

1 | INTRODUCTION

One of the greatest challenges in materials science is to understand how supramolecular structures self-assemble with the desired shape, size, and stability because, in order to achieve this, it is necessary to regulate the physicochemical and conformational properties of their components. In this review, we will focus on polypeptide materials comprising a long chain of amino acids linked by peptide bonds. The ability of these systems to undergo supramolecular self-assembly (SA) is determined by the sequence of primary amino acids that determine the noncovalent intermolecular interactions. Moreover, the ability to design customized supramolecular architectures with adjustable properties opens up a wide range of possibilities for subsequent applications.

In the complete and interesting review by Whitesides, the concept of SA is defined in a general way as "autonomous organization of components into patterns or structures"[1] whereby these structures have a higher order when arranged than as isolated components.[2] Structures self-assembled at the nanoscopic level can be of various sizes, ranging from a few tens to several hundreds of nanometers. The main interactions found in these types of structures are weak forces that act locally and preferably noncovalently (hydrogen bonds, van der Waals forces, π–π stacking interactions, capillarity, and electrostatic and hydrophobic interactions). Moreover, depending on the different forms, chemical compositions and functionalities that are desired to be achieved, atoms, molecules, or a wide range of structures, can be used as building blocks. In addition, the way in which the aforementioned interactions between these blocks are established may result in different structures with specific geometries and dimensionalities,[3,4] including tubular structures, vesicles, liquid crystal phases, micelles, bilayers, or Langmuir monolayers.[5–7]

As we have mentioned before, one of the main characteristics of self-assembled systems is their great dynamism and the fact that they are obtained as a result of these weak interchain interactions, which are capable of reorganizing and adapting to the environment that surrounds them, thus endowing these systems with reversibility and an inherent ability to self-correct when errors are detected.[8] Therefore, to achieve stability in these structures, it is necessary that these interactions act synergistically and cooperatively such that it is more thermodynamically favorable to maintain the self-assembled structures than their decomposition into individual components.[9–11]

Living systems are made up of natural components that present great complexity and, as such, tend to be multifunctional and constantly changing. In light of this, many researchers have been inspired to mimic the physicochemical properties of these natural systems to obtain new and more sophisticated systems that can be used to improve people's lives in numerous fields of application both within medicine as well as nonmedical applications.[12] For example, the biomaterials manufactured today are rich in information and incorporate biologically active components derived from nature with dynamic behavior.

The conformational flexibility of these disordered systems arises due to the lack of restrictions on the degrees of freedom necessary to form structured assemblies with specific conformations, which implies a change in the traditional concept of structure-function dependency.[13] There has been great progress in the field of biomaterials due to the fact that numerous protein molecules and/or domains that continue to fulfill their functions even when partially structured, or completely disordered, in solution have been found.

In recent years, the science of proteins and its main dogma that associates the three-dimensional (3-D) structure of proteins with their final function has changed because of the numerous intrinsically disordered proteins (IDPs) found naturally and with great functional importance. These IDPs are hybrids containing both ordered and intrinsically disordered protein regions (IDPRs).[14] Unlike globular proteins, whose fundamental characteristic is the presence of well-structured and formed domains thanks to the cooperation of various forces, IDPs lack cooperatively folded structures under native conditions.[15] However, there is a wide range of protein structures, ranging from fully unstructured or random-coil-like structures to partially structured in the form of a premolten globule (PMG) and molten globule (MG), rather than a single specific state.[16] Different functional modules, such as short-length fragments, consisting of 3–10 amino acids, also known as short linear motifs (SLiMs, LMs, or MiniMotifs), which can appear several times in the same protein, are found within IDPRs. Other types of longer peptide motifs, known as preformed structural elements (PSEs), comprising 10–70 amino acids, and molecular recognition features (MoRFs), characterized by being linear in the protein sequence, are also included.[17]

The main characteristic of these IDPs and IDPRs is that they maintain their functionality despite lacking a single and orderly structure. They can be found in all organisms and perform vital functions in numerous biological processes, complementing the functions of ordered domains. The functions associated with these IDPs can be grouped into four broad classes: molecular recognition, molecular assembly, protein modification, and entropic chain activities.[18] Indeed, these regions are so important that mutations in their sequences lead to the onset of numerous diseases and conditions in humans.[19] The flexibility and plasticity inherent to disordered regions arise due to their low sequence complexity and biased amino acid composition, as well as their high percentage of charged and hydrophilic amino acids and low percentage of bulky hydrophobic amino acids. Thus, this state remains unfolded thanks to the high net charge and low average hydrophobicity, thus reducing the hydrophobic effects that favor folding of peptide into compact tertiary structures.[20,21] Proline (P) has been shown to be the amino acid that promotes most protein disorder, followed by glutamic acid (E) and serine (S). This is due to the fact that proline is unable to form stabilizing hydrogen bonds in secondary structures because it has a more rigid cyclic structure than other amino acids.[22,23] The presence of proline in the polypeptide chain has a great influence in determining what the final conformation of the secondary structure will be, especially when it is combined with glycine. Thus, when proline is present in IDPs and IDPRs, it tends to establish nonclassical conformations, such as the type II polyproline helix (PPII).[24]

The structure is highly flexible in this unfolded state, thus allowing it to respond to different stimuli and interact with different targets, folding into different dynamic molecular assemblies[25–27] that can undergo phase changes.[28] Conditional transitions between ordered and disordered states triggered by intrinsic and extrinsic factors allow proteins to switch between conformational states, thereby enabling various protein functions.[29] In this review, we will describe the use of elastin-like recombinamers (ELRs) as IDPs in different applications, including self-assembling systems and chemically cross-linked systems.

2 | ORDER–DISORDER IN NATURE

As mentioned previously, IDPRs are common in eukaryotic proteins. In fact, some studies report that almost half of the eukaryotic proteome contains small sequences of 40 or more amino acids, which present disorder under physiological conditions.[27,30]

Uversky has published a comprehensive review of the (meta) physics of the "mysteries" of intrinsic disorder and how these IDPs are able to adopt highly unlikely structures for ordered proteins in order to maintain their biological activity. Indeed, not only has a new group of biologically active proteins been recognized, but it is also clear that these proteins/regions are highly prevalent in nature.[14]

The extracellular matrix (ECM) comprises different proteins and proteoglycans, which form a 3-D network that performs specific structural and biological functions. The predominant extracellular proteins include collagen (which is the most abundant protein in the human body), laminins, elastin (and their associated proteins such as fibulins and fibrillins), and fibronectin. All these structural proteins are attached in a particular way in molecular and supramolecular assemblages, thus providing the shape, organization, and mechanical properties characteristic of tissues.[31] The ECM also contains complex polysaccharides known as glycosaminoglycans, including dermatan sulfate, heparan sulfate, chondroitin sulfate, keratin sulfate, and hyaluronan. With the exception of hyaluronan, all of these bind covalently to proteins to form so-called proteoglycans.

Many biological processes need extracellular proteins enriched in disordered regions to carry out their functions, such as the interaction between the ECM and receptor, interaction with integrins, and adhesion between cells and the matrix or focal adhesions. The proteins in the ECM are assembled into molecular and supramolecular assemblages in a particular way, presenting various states that promote different interactions between proteins and glycosaminoglycans ECM and the cell surface. Moreover, some of them may present posttranslational modifications as a result of hydroxylation or glycosylation (such as collagens or proteoglycans). Peysselon et al.[31] realized that many of the structural proteins in the ECM share functions with proteins that are intrinsically disordered, so they decided to perform a large-scale computational analysis to study the degree of intrinsic disorder of human extracellular proteins. To do this, they turned to the UniProtKB database and predicted the disordered residue index for each protein sequence using the IUPred web server.[32,33] They were able to calculate the percentage intrinsic disorder for each protein by calculating the percentage of disordered amino acids with respect to the total number of amino acids. The results they obtained are very revealing, because 26.7% of the human extracellular proteome (244 proteins), 18.3% of the human secretome (a set of 1800 proteins secreted within the ECM), and 23.2% of the human proteome (20 235 proteins) contain disordered residues. As such, it can be seen that the human extracellular proteome contains, on average, a higher percentage of disorder than the human secreted proteome and the complete human proteome. These authors also found that 21.7% of human extracellular proteins contain more than 50% disordered residues, compared with only 16.3% in the human proteome. Thus, the extracellular proteome is enriched in highly disordered proteins (>50% disorder). Finally, they concluded that 57.4% of extracellular proteins and 45.5% of human proteins contain at least one sequence of 30 consecutive disordered residues, compared with 31.2% of extracellular proteins, and only 18.2% of human proteins contain at least one sequence of 100 consecutive disordered residues. These long protein regions are what make the extracellular proteome enriched in disorder. This group was also able to estimate the degree of disorder for ECM proteins. For example, they concluded that laminins contain less than 20% disordered residues, the proteins that form elastic fibers and proteoglycans vary between 21.8% and 25.8%, and collagens contain more than 50% disordered residues. The disorder in these ECM proteins is mainly due to the sequences folded into a polyproline II helix, which is rich in acidic amino acid residues. Generally, the ECM proteins that are responsible for providing tensile strength to tissues are very disordered, and it is likely that this intrinsic disorder provides peptide chains with the structural plasticity necessary for SA and the ability to interact with different systems in different tissues, thus obtaining a specific tissue organization in the ECM.[31]

The development of reliable prediction tools and databases has provided the opportunity to determine the frequency of intrinsic disorder in both IDPs and IDPRs at the proteome level. Thus, long IDPRs of more than 40 consecutive residues were initially predicted to be present in more than 15 000 proteins, and very long disorder sequences were found for more than 1000 proteins.[34] An exhaustive study of the proteins encoded by 31 genomes from the three kingdoms of life determined that eukaryotic cells have a higher level of disorder than prokaryotic cells and archaea.

Eukaryotic cells have numerous compartments lacking a surrounding membrane on a micrometer scale, known as biomolecular condensates, in which specific nucleic acids and proteins are concentrated. These compartments have been found in the nucleus, cytoplasm, and membranes of virtually all eukaryotic cells. These biomolecular condensates behave as separate phase liquids and are enriched in multivalent molecules that are responsible for establishing intra- and intermolecular interactions.[35] These molecular condensates are liquids that are formed as a result of liquid–liquid demixing (phase separation) of the surrounding cytoplasm. The existence of a phase boundary explains how molecules can concentrate in a particular place in a cell without a surrounding membrane and still provide a suitable environment for cellular biochemistry that depends on rapid diffusion

and allows for a chemical balance between compartments of different chemical properties (such as concentration) via the rapid movement of molecules between them.

Molecules that are frequently enriched in biomolecular capacitors include proteins containing large IDPRs because they can phase-separate themselves under physiological conditions. This is due to the fact that IDPRs contain repetitive sequences, generally aromatic residues, which allow intermolecular cation–π interactions with Arg residues and π–stacking interactions.[28] In addition, phase separation is also promoted by sequences enriched in Gln, Asn, and Ser residues as a result of dipolar interactions with their side chains.[36] Finally, IDPR-rich proteins can separate into phases when blocks with oppositely charged residues interact, either between two different molecular types or as alternating blocks in the same molecule.[35] All these types of interactions (aromatic, polar, and charge–charge) are of short duration and promote the structural dynamism that exists in phase-separated liquids.

Initially, due to the structural requirements necessary for enzymes to perform their catalytic function, these enzymes were excluded from the group of IDP and IDPR proteins. Recently, however, DeForte and Uversky[37] found that enzymes contain regions with specific IDPR lengths with specific functions. In addition, it was found that prokaryotic enzymes present less disorder than eukaryotic enzymes, thus showing that this disorder is related to functional and structural complexity. The free-energy profile of an IDP is relatively simple and flat and is extremely sensitive to environmental changes. This would explain the conformational plasticity of IDPs and IDPRs, their great sensitivity to changes in the environment, their ability to interact with different molecules, and, consequently, their relative ease to fold into different 3-D structures.[38,39]

The most widely used techniques to determine and characterize the disorder and the assembly model can be divided into computational or experimental techniques, especially computer simulations based on polymer physics, single-molecule fluorescence energy transfer (smFRET), X-ray crystallography, small-angle X-ray scattering (SAXS), or nuclear magnetic resonance (NMR) spectroscopy.[15]

3 | ELASTIN-LIKE RECOMBINAMERS

Elastin is one of the major components of the ECM and is especially abundant in those tissues that require numerous relaxation and stretching cycles, such as the skin, ligaments, blood vessels, or lungs. Elastin gives these tissues properties such as resistance and elasticity, as well as the ability to regulate various cellular activities, such as adhesion, migration, proliferation, and differentiation.[40,41] Natural polymers have a predetermined structure; therefore, the degree to which they can be modified and functionalized to obtain desired end properties is limited. For example, natural elastin is an insoluble polymer synthesized from its precursor, tropoelastin. This limitation is the main reason why genetic engineering and recombinant technologies have recently been used to obtain polymers with a controlled synthesis.[42] This recombinant synthesis allows the production of materials with a specific amino acid composition. Likewise, it allows biofunctional or bioactivity sequences to be included. Additionally, recent advances in expression systems and recombinant DNA techniques have demonstrated the feasibility of large-scale production.[43]

In the 1990s, Urry et al.[44] presented the exhaustive work they had performed to develop elastin-like polypeptides (ELPs) in numerous publications. These polymers were inspired by the composition of elastin. More recently, a new nomenclature was introduced for ELPs produced using recombinant techniques to highlight their origin and differentiate them from materials obtained directly from natural sources. This new terminology defines recombinantly obtained ELPs as ELRs.[45]

ELRs are based on the highly repeating hydrophobic domains of natural elastin. These domains mainly comprise the amino acid residues glycine (G), valine (V), and proline (P) and are generally found as GV, PGV, and GGVP or GVGVP blocks.[46,47] However, the most widely used and studied characteristic structure is the pentapeptide $(VPGXG)_n$, where "X" is a guest residue, which can be any amino acid except proline and "n" is the number of repeats of the pentapeptide. The choice of host amino acid is what determines the physicochemical and mechanical properties that the recombinant polymer will have, and therefore, it is the key element to take into account when designing a new ELR.[46,48] ELRs exhibit a smart temperature responsive behavior, undergoing a reversible phase transition, known as the inverse temperature transition (ITT), at a characteristic transition temperature (T_t).[49,50] The ITT process has been studied for model ELRs and has been described as the phase separation between water and ELR molecules above that T_t, driven by the difference in the entropy of the system in both states. In an aqueous medium, the ELR chains are fully hydrated below T_t, mainly as a result of hydrophobic hydration, and the polymer is soluble. However, above this T_t, the ELR reversibly assembles hydrophobically and undergoes a phase transition into two different phases—water-rich and polypeptide-rich—in which the ELRs lose the water surrounding the hydrophobic groups such that a phase-separated state is formed, precipitating and establishing a regular, dynamic, nonrandom structure characterized by the presence of type II β turns. The T_t depends mainly on the mean polymer polarity and, thus, is dependent on the nature of the guest residue. As such, T_t increases as hydrophobicity decreases and vice versa. However, other factors, such as pH, temperature, ionic strength of the solution, light, polymer concentration, or the presence of other cosolutes, can also affect the coacervation process.[51–53] The most commonly used techniques to study ITT are differential scanning calorimetry (DSC) or turbidity.

4 | ELRS AS IDPS

Numerous protein-based polymers can perfectly mimic these IDPs and IDPRs.[54] Some of the most prominent are ELRs, the sequences of which can be tailored to meet the desired need, as already mentioned above, thanks to their recombinant nature. These polymers also have a high concentration of proline/glycine amino acid

sequences[55] and exhibit a reversible transition phase that depends on the specific conditions of pH, pressure, or temperature.[47]

The essential property of elastin is the reversible elastic ability arising due to its hydrophobic domains.[56] A common feature between ELRs and IDPs is the high number of tandem proline and glycine repeats with limited hydrophobicity and low amino acid sequence complexity.[21] As such, it has been proposed that the structural disorder in ELRs is due to the high content of proline and glycine in the ELR backbone, because both these amino acids help to keep the polypeptide structure of elastomers disordered and hydrated. Proline is a very rigid amino acid and, as such, does not allow the formation of hydrogen bridges within the same backbone, thus preventing the formation of common secondary structures such as α-helices and β-sheets. In contrast, the absence of a side chain in the amino acid glycine allows the ELR to present a great variety of chain conformations in the presence of water, which does not favor the formation of ordered structures.[15,57,58]

The ability to control disorder within ELRs plays a fundamental role for the development of new biomaterials and their subsequent use in biomedical applications. Such applications include studies related to biomineralization. Thanks to the fact that ELRs present great flexibility when self-assembling into different conformations, different varieties of structures that are capable of controlling biomineralization can be obtained.[59–61] For instance, Li et al.[62] have reported bone fibrils made using an ELR similar to those made of collagen that are capable of carrying out an intrafibrillar mineralization process due to their ordered structure.

The balance between order and disorder is also very important when varying the mechanical properties of ELR hydrogels to mimic the mechanical properties of the native tissues concerned. For example, Roberts et al.[63] developed a new biomaterial based on alternating ordered polyalanine motifs with inherently disordered ELR domains to produce injectable porous hydrogels. The versatile composition of these ELR-based polymers, as well as their varied functions, allows these biomaterials to be used as covalent coatings in numerous biomedical devices that are permanently in contact with the human body. For example, biofunctional sequences can be introduced to improve the biocompatibility of coated biomedical devices by preventing rejection of the biomaterial after implantation or avoiding the appearance of subsequent infections. Along these lines, Acosta et al.[64,65] reported new amphipathic biopolymers with antimicrobial and immunomodulatory properties and the ability to self-assemble into supramolecular nanostructures. These biomaterials comprised an antimicrobial peptide (AMP) and an ELR that is able to self-assemble in order to develop supramolecular nanomaterials via a dual assembly process. The process begins with the formation of nanofibers by the AMP domains and subsequent formation of fibrillar aggregates thanks to the thermally triggered response of the ELRs. Both SA domains were useful for driving the hierarchical organization of intrinsically disordered protein polymers (IDPPs).

Thanks to this ability to choose the desired guest residue and design different sequences, including bioactive sequences, different structures can be obtained, depending on the final application. Thus, hydrogels, particles, micelles, surface coatings, porous scaffolds, and films can be formed.[66] In the following sections, some of these structures will be studied, along with their application as IDPs within ELRs.

5 | SELF-ASSEMBLED IDPS-BASED NANOSYSTEMS

5.1 | Di- and multiblock copolymers

5.1.1 | Vesicular systems-nanoparticles

Vesicles are self-assembled functional structures that can be used for different biomedical applications, ranging from microbioreactors to drug delivery.[67–69] The main components that have been used to form vesicles by molecular SA are amphiphilic phospholipids or diblock copolymers. Biological liposomes or lipid-based vesicles are the most abundant in nature. However, they present some limitations that affect their applicability due to their instability and limited shelf life. To overcome these limitations and improve the mechanical properties and stability of biological liposomes, synthetic polymeric vesicles known as polymersomes,[70] which allow the size, shape, and permeability to be varied, were developed. However, these polymeric vesicles also presented disadvantages such as low biodegradability, biocompatibility, or biofunctionality. Finally, to address these limitations, modulable vesicles have been developed using recombinant proteins. Numerous examples of constructs with amphiphilic blocks based on proteins that have been assembled into different supramolecular structures, such as vesicles[71–74] or micelles,[75–77] have been described in the literature for many different applications.[76,78–81]

The protocols used to form the assembled structures often lack biocompatibility, assembly control, or encapsulation efficiency. Consequently, Schreiber et al.[82] developed a new protocol for the controlled SA of amphiphilic ELRs ranging from spherical coacervates to stable unilamellar vesicles, depending on the conditions used. Robust and optimized assembly protocols produced vesicular protein membrane-based compartments (PMBCs) with adjustable size, high efficiency, surface loading, and stability. These amphiphilic ELRs contain hydrophobic (rich in the amino acids phenylalanine [F] and isoleucine [I]) and hydrophilic domains (rich in the amino acids arginine [R] and glutamic acid [E]) with defined SA properties. To study the different SA behaviors, the proportions of these hydrophobic and hydrophilic domains were varied. As expected, the stability and solubility were found to depend on the physicochemical properties of the side chain in the inserted guest residue. Phase separation, which is achieved by mixing organic solvents with water, is required to obtain these supramolecular and bilayer structures. Two different methods were used in this article to obtain micelles. The first of these was based on the tetrahydrofuran (THF) swelling method in which fibrous, spherical, and vesicular structures are formed irrespective of the charge and the other, more successful method involved *n*-butanol (BuOH) extrusion in which the vesicular structures are formed irrespective of the temperature. The formation of vesicular structures requires an osmotic pressure

equilibrium between the outside and the inside of the structure to obtain a stable vesicular architecture. This second and more advantageous method for obtaining vesicles avoids the formation of fibers and spherical coacervates. Subsequently, these authors verified the effectiveness of encapsulating various molecules, ranging from small hydrophilic and hydrophobic molecules to large folded proteins, thereby highlighting the potential use of these vesicles for controlled drug administration.

Taking a further step in the development and application of these amphiphilic vesicles, Schreiber et al.[83] used them as prebiotic compartments because they are able to imitate membranes based on lipid bilayers. Thus, these authors created a model for prebiotic protocells based on stable dynamic protein membranes that adapt to anabolic reactions using self-assembled dynamic PMBCs containing repeats of simple pentapeptides, namely, amphiphilic peptides comprising only prebiotic amino acids. Three functional molecular species are required in order to obtain a prebiotic protocell: catalysts, information storage molecules capable of replication, such as RNA, and compartment-forming molecules. These amphiphilic proteins could assemble into dynamic protein membranes and thus form compartments. The amphiphilic diblock proteins can be obtained by the repetition of pentapeptides comprising only four prebiotic amino acids, such as $(VPGHG)_{20}(VPGIG)_{30}$ or $(VPGHG)_5(VPGLG)_4$, that are assembled into PMBCs in vitro. These PMBC protocells are very stable and able to withstand extreme conditions of temperature, pH, and ionic strength. Furthermore, encapsulation of small molecules or macromolecules within PMBCs can be carried out. For this purpose, small hydrophobic dyes (FM4-64), positively charged hydrophilic dyes (Rho 13), and polymeric glucose (Dextran Red) were encapsulated in the vesicles formed using the BuOH extrusion method, in addition to large molecules such as intact proteins (GFP). All these molecules were incorporated into the vesicular lumen during PMBC assembly. It was only possible to encapsulate the positively charged hydrophilic dye (Rho 13) and polymeric glucose (Dextran Red) in the vesicles formed using the THF swelling method. Furthermore, they were found in both the vesicular lumen and the PMBC membrane. As a result of these methods, advanced nanoreactors could be formed in the future for drug delivery by controlling the loading of their components.

Along similar lines, Hassouneh et al.[84] have performed a theoretical study of the SA of ELR diblock copolymers to form weak micelles with a dense core and almost unstretched coronas, a state not previously observed for synthetic diblock copolymers: synthetic diblock copolymers usually form strong micelles. This new micellar state is due to the close control of the amphiphilicity of these synthetic recombinant peptide copolymers. To determine the type of micelle to be formed (weak or strong) theoretically, three contributions to free energy that come from the corona, the interface, and the core must be studied. In this theoretical model, the interactions at the core of the micelle are significantly stronger than the interactions at the core–corona interface. Hence, weak micelles have a very compact core and an almost unstretched corona, which leads to a low surface tension. In contrast, strong micelles have a less compact core with a fully stretched corona, which leads to a high surface tension (Figure 1). Six ELRs with different lengths of the hydrophobic and hydrophilic blocks were studied in order to self-assemble them into spherical micelles. The ELRs considered in this work comprise a hydrophilic block containing valine (V), glycine (G), and alanine (A) guest residues in a ratio of 1:7:8, whereas the hydrophobic block contains only valine (V) as guest residue. The presence of valine in different percentages in both blocks provides amphiphilicity to the polymer. Below the critical micelle temperature (CMT), ELR diblocks are soluble as unimers, with SA of these ELR diblock copolymers occurring above the CMT. The hydrophobic blocks form the core of the micelles while the hydrophilic blocks remain hydrated and form the corona of the micelles. Upon further heating, the hydrophilic blocks also become insoluble, and the ELR diblock phase separates. As such, these authors presented a new theoretical model that predicts that weak ELR diblock copolymer micelles are formed due to their composition, and variations in the sequence lead to a decrease in the core–corona surface tension, with stronger interactions being formed in the core of the micelles.

Taniguchi et al.[85] have studied the behavior in self-assembling of short aromatic containing elastin-derived peptides, formed by $(XPGVG)_3$ where X is an aromatic acid as tryptophan, tyrosine, or phenylalanine. They have determined the importance of aromaticity and hydrophobicity for their coacervation, and they have proposed that these aromatic amino acids can participate in intermolecular

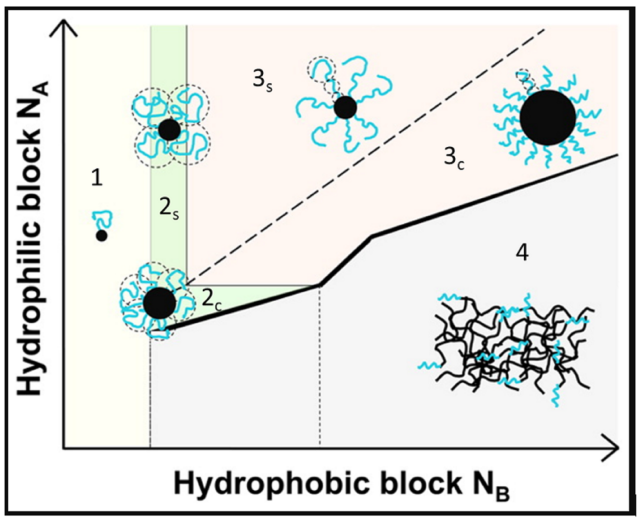

FIGURE 1 Diagram represents the different states of aggregation of elastin-like recombinamer (ELR) diblocks made up of a hydrophobic block (N_B) and a hydrophilic block (N_A). In Region 1, the ELR diblocks are found as isolated unimers. In Region 2, the formation of weak micelles (weak star-like micelles [2_s] or weak crew-cut micelles [2_c] depending on N_A) occurs with a very compact core and an almost unstretched corona, which leads to a low surface tension. In Region 3, the formation of strong micelles (strong star-like micelles [3_s] or strong crew-cut micelles [3_c] depending on N_A) occurs with a less compact core with a fully stretched crown, which leads to a high surface tension. Finally, in Region 4, the ELR diblocks self-assemble into nonspherical morphologies or separate into two-phase solutions. Adapted with permission from Hassouneh et al.,[84] Copyright (2015), American Chemical Society

π/π and CH/π interactions that enhance their coacervation property. In fact, $(WPGVG)_3$ provided a more potent coacervation than tropoelastin (approximately 63 kDa) because it is derived from the indole group which is very hydrophobic and with a large π-system. In further work from Suyama et al.,[86] different elastin-derived peptides were chemically synthesized using the solid phase method to study the effects of forced dimerization on coacervation. The new peptides obtained were the Cys-$(FPGVG)_5$ (N-dimer) and $(FPGVG)_5$-Cys (C-dimer) homodimers and the Cys-$(FPGVG)_5$ coupled to $(FPGVG)_5$-Cys heterodimer. By means of turbidimetry, they verified that the T_t of the three new dimers was close to 14°C, while on the contrary, the monomer $(FPGVG)_5$ presented a T_t of 38°C. Therefore, they corroborated that the dimerization of these peptides improves the coacervation capacity with respect to the monomer $(FPGVG)_5$. In addition, through the simulation study of molecular dynamics (MD) and the measurement of circular dichroism (CD), it was verified that these dimers have a sheet-turn-sheet type structure. Each dimer and monomeric peptide had a common characteristic motif consisting of a consecutive sheet (Gly-Val-Gly), turn (Phe-Pro-Gly-Val), and sheet (Gly-Phe-Pro) that are stabilized by hydrogen bonds between the first sheet (Val) and the second sheet (Phe) and a hydrophobic interaction between two Pro residues. In these dimers, there are two hydrophobic domains that are used to bind the peptides together, and this accumulation of hydrophobic domains favors the coacervation of the dimers compared with monomer $(FPGVG)_5$ occurring at a lower temperature and concentration. In a related work to the aforementioned, the same authors[87] studied the improvement in the coacervation of nonlinear elastin-derived peptides [cyclo$(FPGVG)_n$, $n = 1–5$] thanks to a simple cyclization favoring self-aggregation. Furthermore, they found that cyclo$[FPGVG]_5$ coacervate is able to retain dye molecules, making this material an ideal candidate for controlled drug delivery.

5.1.2 | Multiblock

In another study, MacEwan et al.[88] developed and characterized new multiblock copolypeptides based on ELRs by keeping the final length of the chain constant but systematically varying the size, type, and distribution of the blocks along the polypeptide chain, thus forming what is known as a block architecture. These authors found that, depending on the architecture of these multiblocks, the properties of the resulting copolypeptides could vary. Eleven ELRs with unique block architectures, in which the length and distribution of hydrophobic and hydrophilic blocks varied, were developed. Each ELR comprised the 60 pentapeptide repetitions of the hydrophobic monomer (VPGVG) and the 60 pentapeptide repetitions of the hydrophilic monomer (VPGSG). The organization of these pentapeptides along the polypeptide chain was varied, thus obtaining ELRs with different structures, such as the homopolymer, alternating copolymer, diblocks, triblocks, and gradient copolymers (ELP-SVG_L, ELP-SVG_I, and ELP-SVG_H), This new concept of gradient copolymer was developed so that the sizes of the blocks changed gradually along the polypeptide chain. In this way, different gradients of composition are obtained, which are denominated ELPs with low gradient (ELP-SVG_L), intermediate gradient (ELP-SVG_I) or high gradient (ELP-SVG_H). The pure hydrophilic/hydrophobic terminal blocks of these gradient ELPs were 25.0%, 29.2%, or 33.3% of the total ELP length and, respectively, 30, 35, or 40 pentapeptides. The results showed that homopolymeric ELRs and alternating ELRs are soluble below their T_t and coacervate into insoluble aggregates above T_t. However, ELR diblock copolymers comprising two blocks with different T_ts can self-assemble into spherical micelles above their critical micellar temperature (CMT) after selective coacervation of their most hydrophobic block. Finally, each gradient copolymer exhibits novel thermal behavior. Thus, whereas ELP-SVG_L did not exhibit nanoscale SA and only exhibited a unimer-to-aggregate phase transition at a T_t very close to that measured for the alternating block copolymer ELP_S, ELP-SVG_I and ELP-SVG_H exhibited two independent temperature-triggered transitions—a unimer-to-micelle transition and a micelle-to-aggregate transition—at higher temperatures. Therefore, the authors of this study concluded that the morphology and size of polypeptide micelles can only be modified by controlling the architecture of the blocks; in other words, SA of the polypeptide can be modulated by varying the sequence of the multiblocks, verifying that the micelles with a higher radius are those in which there is a gradient and in which the hydrophobic and hydrophilic blocks are longer and located at the ends of the polypeptide.

ELRs can self-assemble into physically cross-linked hydrogels above a certain transition temperature in the case of smart elastin-like tetrablock-copolymer structures.[89] In this regard, a multifunctional ELR hydrogel has been developed by Coletta et al.[90] from two bioactive ELRs, one including the RGD cell-adhesion domain (ELR-RGD) and the other including the osteogenic and osteoinductive factor BMP-2 (ELR-BMP) and both of them including an elastase sensitivity resulting from repetition of the VGVAPG hexapeptide.[91] The hydrogel was found to be biodegraded by enzymatic cleavage, simultaneously releasing BMP-2, thus meaning that this hydrogel acts as a controlled drug-delivery system. On the other side, the potential of these multifunctional hydrogels in bone regeneration was studied in a pilot study involving a femoral bone injury model in New Zealand White rabbits consisting of the creation of a defect 6 mm in diameter in a femoral condyle 8 mm in diameter and subsequent filling of the defects with the hydrogel. The hydrogel biodegraded as a result of elastase (MMP-12) secretion by osteoclasts while simultaneously promoting bone formation, and this resorbable matrix maintained bone integrity until full regeneration. The RGD sequences helped migration and proliferation of cells inside the scaffold, favoring bone neo-formation at the femoral injury, as confirmed by computed tomography, radiography, and histology. Therefore, the BMP-2-loaded hydrogels were found to be biodegradable, cytocompatible, and injectable and avoided the need for scaffold removal after bone regeneration, showing complete defect regeneration in six out of seven cases, with the other showing partial closure of the defect.

5.2 | Incorporation of additional order- and disorder-promoting peptide/protein domains (controlled secondary structure)

5.2.1 | α-Helical coils: Collagen-like and leucine zippers

This section is devoted to those IDPRs that promote α-helical coil formation, including those mimicking collagen, which is another major component of the ECM, and those acting as zippers. Different types of collagens perform vital functions in biological activities such as cell migration, cell adhesion, tissue scaffolding, or tissue repair.[92] However, although these different collagens perform different functions, they all share the same tertiary structure, namely, a collagen triple helix comprising three polyproline-II type right-handed helices. As with elastin, the limitations of animal collagen, such as thermal instability and possible contamination with pathogenic substances, have led researchers to develop synthetic models of collagen, better known as collagen-like peptides (CLPs). CLPs are short synthetic peptides that mimic the characteristic triple-helix conformation of native collagens. The repeating motif on each strand of the helix consists of a glycine (Gly)-X-Y tripeptide in which the X and Y residues are generally proline (P) or hydroxyproline (HyP). Unlike full-length native collagens, these CLPs exhibit reversible triple-helix folding and unfolding as a result of their relatively low molecular mass.

The α-helical coil is known to be responsible for oligomerization in a wide spectrum of proteins.[93] In this regard, the so-called leucine zippers (Z) are an interesting group of α-helical domains[94] characterized by heptad repeating units designated "abcdefg," where the "a" and "d" positions are occupied by hydrophobic residues such as leucine and the "e" and "g" positions are occupied by charged residues.[95] Each spiral domain folds into an amphiphilic α-helix that places the "a" and "d" residues on a hydrophobic face, with hydrophobic interactions causing these helixes to associate in a spiral.[96]

Zippers

Vesicles that are assembled from folded globular proteins have been found to be able to carry out different functions than traditional lipid or polymeric vesicles.

Along these lines, Jang et al.[97] developed a new strategy for the design of protein vesicles containing functional globular domains. Recombinant globular fusion proteins containing leucine zippers and ELPs are used to form these new vesicles by tunable SA. As a result of in-depth study of the SA process, which is dependent on temperature and concentration, these authors were able to adjust both the size and structure of globular protein vesicles. Two different recombinant fusion proteins were designed to spontaneously form these globular protein vesicles or "globule-zipper-ELR" complexes. The first fusion protein (ZR-ELP) consists of an arginine-rich basic leucine zipper (ZR) and a thermo-sensitive ELP, whereas the second fusion protein (mCherry-ZE) is made up of a globular fluorescent protein (mCherry), which serves as a functional model protein, fused with a glutamic acid (ZE)-rich leucine zipper. These fusion proteins are capable of forming reversible complexes in solution as a result of the high affinity binding of leucine zippers and the reverse phase transition that ELPs undergo upon changing the temperature. This thermal driving force, which can be controlled by varying the protein concentration or temperature, is responsible for controlling the size of the vesicles, as well as whether the vesicles have one or two layers. Thus, vesicles with only one layer are formed due to the steric hindrance of the globular groups of mCherry, which are present in the membrane, and to the limitations derived from the rigid structural conformation of leucine zippers, whereas bilayer vesicles are formed when the temperature is increased, which leads to an increase in the hydrophobicity of ELPs, thereby inducing stronger inter- and intramolecular interactions of ELPs. One of the main advantages of this intelligent and biocompatible SA is that it allows the direct incorporation of globular proteins into vesicles without needing to use denaturing solvents, thus maintaining the specific bioactivity of the inserted globular domain. Furthermore, they are capable of selectively encapsulating both hydrophobic and hydrophilic fluorescent dyes to directly visualize the molecularly organized structures in the vesicle membrane and determine whether these vesicles are made up of one or two layers. These authors used rhodamine octadecyl ester perchlorate B (RhoB) as a model hydrophobic lipophilic dye to verify the location of the hydrophobic ELP domain, with calcein as a hydrophilic model dye to identify water-rich regions.

Along similar lines, and with regard to the use of leucine zippers, Fenández-Colino et al.[98] developed a new ELR biomaterial containing a leucine zipper sequence, thus giving rise to a recombinamer known as a leucine zipper-elastin-like recombinamer (ZELR), that allowed them to study the behavior of both sequences when they coexist in the same polypeptide chain. Subsequently, this new recombinant biomaterial (ZELR) was used to develop new hydrogels that have the characteristics of being stable, reversible, and injectable, thus making them excellent candidates for use in tissue engineering. This new polymer is designed in a single recombinant molecule and is made up of a thermosensitive amphiphilic tetrablock ELR (comprising two hydrophilic blocks containing the VPGEG pentapeptide and two hydrophobic blocks containing the VPGIG pentapeptide) and a leucine Z zipper domain that is able to dimerize. In this design, the Z residues cannot form a network when the ELR is below its T_t, thus guaranteeing that the polymer is dissolved under these conditions. However, when energy is supplied to the system and above T_t, the ELR chains collapse, and the Z domains can interact synergistically with each other, thus forming a stable hydrogel. This study found that the tetrablock alone is not able to form a stable hydrogel, because it loses its integrity when in contact with an aqueous medium and goes from a physically cross-linked hydrogel to a micellar dispersion. However, when the leucine zipper domain is added, this dispersion is corrected, thus giving rise to stable hydrogels thanks to the positive cooperative effect in which the interaction between both the Z and ELR residues results in a greater stability of the whole than that shown by independent systems.

Collagen-like

As mentioned above, CLP triple helixes have recently been used as physical cross-linkers in CLP biopolymer hydrogels with a predesigned thermo-responsiveness. This is due to their ability to attack native collagens via triple helix hybridization, thus leading to the formation of new CLP-polymer and CLP-peptide conjugated biomaterials displaying well-defined nanostructures. In this regard, several studies that combine ELPs with collagen in order to improve the properties of these new biomaterials by combining the benefits of elastin with the benefits of collagen, and their possible application in tissue engineering or targeted drug administration, will be highlighted.[92]

Prhashanna et al.[99] examined what happened to the ELR transition temperature, T_t, when the guest residue (X) is varied in the pentapeptide sequence $(VPGXG)_4$ of the short ELPs, both in the free state and when this ELR is conjugated with CLPs. To that end, they studied three different ELP biopolymers: the first ELP was a repetition of the amino acid tryptophan $(VPGWG)_4$, the second ELP was a repetition of the amino acid phenylalanine $(VPGFG)_4$, and the last ELP was a combination of both amino acids (VPGFG)(VPGWG)(VPGWG)(VPGFG). These authors found that, for the first two ELP biopolymers ($(VPGWG)_4$ and $(VPGFG)_4$), T_t remained constant for both the free ELP and the conjugated ELP-CLP system. The tryptophan-based ELPs exhibited a lower T_t than the phenylalanine-based ELPs, probably because tryptophan has a more voluminous aromatic group in its side chain that increases the rigidity of ELP chains, thus leading to less loss of conformational entropy upon aggregation and, therefore, a lower T_t. However, when these two amino acids were combined in the same polymer ((VPGFG)(VPGWG)(VPGWG)(VPGFG)), there was a change in T_t when they changed from free-ELP (T_t > 353 K, 80°C) to CLP-conjugated (ELP-CLP), (T_t < 278 K, 5°C). This decrease in T_t after conjugation with CLP is due to the stacking of ELP chains, which decreases the entropic loss on ELP aggregation. For the ELP-CLP conjugate, two temperatures must be taken into account in order to form aggregates, namely, the transition temperature (T_t) of the ELP and the melting temperature (T_m) of the CLP triple helix. The CLP triple helix is stable at temperatures below its T_m due to interchain hydrogen bonds formed by three polypeptide chains. The union between the ELP and the CLP causes a decrease in the T_t of short ELPs due to the local crowding of ELPs near to CLPs. Furthermore, the thermodynamics and structure of the CLP triple helix favor the formation of stable self-assembled nanostructures at temperatures below the melting temperature (T_m) of this triple helix and, in turn, above the T_t of ELP.

Using atomistic and coarse-grained (CG) MD simulations, these authors were able to demonstrate how and why the transition temperature of short ELP peptides, in the free state and conjugated with CLPs, changes depending on the choice of guest residues in the pentapeptide VPGXG. These atomistic simulations confirmed that the free tryptophan-based ELP, $(VPGWG)_4$, tends to adopt structures with a larger number of β-turns compared with the free phenylalanine-based ELP, $(VPGFG)_4$, or the free ELP comprising the combination of both ((VPGFG)(VPGWG)(VPGWG)(VPGFG)) at lower temperatures. However, when these ELPs were conjugated to CLP, both ELPs comprising the combination of both phenylalanine and tryptophan and tryptophan-based ELP have a greater propensity to form β-, α-, and π-turns at low temperatures. As such, these changes in the experimental T_t are due to the combined effect of the increase in local stiffness of W compared with F and to the stronger W–W attractive interactions compared with the F–F interactions, thus leading to a change in the onset of aggregation for the free-ELP and conjugated ELP-CLP systems. As such, adjusting the T_t of conjugated ELP-CLP by varying the guest amino acid allows the formation of stable nanostructures in the temperature range between the T_t of the ELP and the T_m of the triple helix and, therefore, the design of nanomaterials that are biocompatible and can be used under biological conditions.

In the study published by Luo and Kiick,[100] self-assembled vesicles comprising elastin-like block copolymers (ELP) conjugated with CLP (ELP-CLP) were developed. This study was aimed at reducing the high experimental transition temperature of short ELPs by conjugating them with a CLP that forms a triple helix. CLP exhibits a melting temperature of 50°C, which allows the formation of a stable triple helix at physiological temperature. The ELP selected for this work consisted of six repeats of the VPGFG pentapeptide. The lower transition temperature of the conjugate (ELP-CLP) allowed the formation of well-defined nanovesicles with a diameter of approximately 160 nm at physiological temperature. These vesicles were able to dissociate at elevated temperatures, despite the LCST-like behavior of the ELP domain, thus resulting in unfolding of the CLP domain. Taking the abovementioned work as a reference, Luo et al.[101] evaluated the potential of using these newly developed vesicles (ELP-CLP) for drug delivery to target matrices with abundant amounts of collagen thanks to the retention of these vesicles on collagen-rich substrates, presumably due to the interactions formed between the triple helixes of collagen. The LCST-like transition of the ELP domain, together with the dissociation of the vesicles at high temperatures, should allow thermally controlled drug release. To do this, they encapsulated a drug (fluorescein as a model of hydrophobic charge) within the ELP-CLP vesicles and, subsequently, carried out a complete controlled release by heating for 3 weeks. These authors analyzed the cytocompatibility of these vesicles by performing cell proliferation and viability studies using both fibroblasts and chondrocytes, with very good results. Thus, the ELP-CLP vesicles did not induce cell (fibroblast or chondrocyte) death at either 24 or 72 h for any of the ELP-CLP concentrations tested, as evidenced by the fact that the percentage of live cells at all ELP-CLP concentrations and all time points was not significantly different from that of untreated cells. Furthermore, no inflammatory responses were obtained, because the activation of macrophage-like cell lines was not observed.

The study published by Willems et al.[102] investigates the influence of the amorphous or crystallizable block on SA of a silk-like triblock polypeptide that was previously designed to encapsulate single DNA molecules to give rise to rod-shaped virus-like particles (VLPs). This polypeptide has a triblock architecture consisting of a long N-terminal amorphous block, a crystallizable middle block, and a C-terminal DNA-binding block. Because the amorphous block is on the outside of a VLP, it is this amorphous block that will determine, to a large extent, the initial biological response of cells and tissues to this

VLP. The triblock polypeptide studied (C-S_{10}-K_{12}) comprises a collagen-like amorphous domain $(GXaaYaa)_{132}$, where Xaa and Yaa are often proline and hydroxyproline, respectively, necessary for colloidal stabilization of the VLP particles; a silk-like middle domain $(GAGAGAGQ)_{10}$, which allows SA into the rod-shaped core of the VLP via stacking on β-rolls; and, finally, a dodeca-lysine domain for binding to the nucleic acid template. Therefore, to study this influence of the amorphous block, SA of the collagen polymer (C-S_{10}-K_{12}) with DNA was compared with a new elastin-like polymer (E_{80}-S_{10}-K_{12}) containing 80 pentamers (GSGVP) in order to have a similar length to that of collagen. Serine was chosen as the guest residue because it is the most similar to collagen (hydrophilic and uncharged). The amorphous block in elastin $(GSGVP)_{80}$ is less hydrophilic than the amorphous block in collagen $(GXaaYaa)_{132}$. Both amorphous blocks in both systems have similar lengths and adopt a random spiral structure in solution. These authors hypothesized that the indirect influence of the nature of the amorphous block on the DNA-binding properties of the artificial viral capsid polypeptides occurs as a result of an effect on the assembly of the silk-like domains into fibrils that mediate binding cooperativity. The collagen polypeptide was found to be more reluctant to undergo fibril formation at low concentrations than the elastin polypeptide due to its higher hydrophobicity. When elastin-like amorphous blocks were studied, DNA was still encapsulated, but the polypeptide-only fibrils were much longer, and their size distribution partially overlapped with that of the encapsulated DNA fibril. In contrast, when collagen-like amorphous blocks were studied, there was a clear distinction between very short polypeptide-only fibrils and much longer fibrils with encapsulated DNA. Thus, increased hydrophilicity translates into larger random coil sizes of the amorphous blocks and stronger intermolecular repulsions between these more hydrated random coils, which are densely packed along the assembled silk fibrils. As such, it was found that the hydrophobicity of the amorphous block, which depends on the chemical nature thereof, is an important variable that determines the assembly of silk polypeptides, both natural and engineered.

5.2.2 | β-Strands: Silk domains and amyloids

One of the possible highly ordered secondary structures adopted by proteins is the beta sheet or beta folded sheet. It is formed by the parallel positioning of two amino acid chains within the same protein in which the N–H groups of one of the chains form hydrogen bonds with the C═O groups from the other. This is a very stable structure that can be formed after the breaking of hydrogen bonds during formation of the alpha helix. When forming the beta sheet structure, the different strands are folded such that the carbon atoms alternate above and below the plane of the sheet, and therefore, the groups present in the side chains in this structure are also found alternately positioned above and below the plane of the sheets. These groups should not be very bulky, so as not to create a steric hindrance that would impede the structure of the sheet. These structures are hydrophobic.

Silk

Silk is a natural biomaterial with a unique combination of elasticity and strength that approaches the mechanical properties of materials such as Kevlar,[103,104] which has driven its widespread use. The applications of silk proteins and engineered silk-like polypeptides are determined by their unique SA behavior, which is controlled by the alternation of crystallizable and amorphous sequence motifs.

Fernández-Colino et al.[105] have designed and produced a new injectable multiblock co-recombinamer based on silk and elastin (silk–elastin-like recombinaner [SELR]) that spontaneously forms a stable physical nanofibrillar hydrogel under physiological conditions. This is an amphiphilic multiblock co-recombinamer (EIS) consisting of a hydrophobic block comprising isoleucines as guest residue and a hydrophilic block comprising glutamic acid as guest residue; the silk domain is $(GAGAGS)_n$. This new material showed a concomitant and coordinated dual gelation mechanism. The gelling process consists of two stages, with an initial reversible rapid gelation (forming micellar structures) thermally driven by the co-recombinamer solution once the system reaches body temperature due to the thermal responsiveness of the elastin-like motifs (ELR) and with the amphiphilic multiblock design of the co-recombinamer being responsible for hydrogel formation. A stage of stabilization, reinforcement, and microstructuring of the gel then occurred as a result of the formation of irreversible beta sheets around the silk motifs (SL). Thus, the hydrophilic blocks, which do not exhibit LCST behavior under the conditions used, are responsible for water retention, whereas the cross-linking function is achieved by the thermally driven folding and hydrophobic interaction of the hydrophobic blocks.

Related to the abovementioned study, Ibáñez-Fonseca et al.[106] developed a new SELR that differs from the previous one in that the ELR domain is based on the combination of lysine and isoleucine, thus showing a slight amphipathicity throughout the whole molecule but still maintaining a strong hydrophobicity due to the burying of lysine-containing pentapeptides within highly hydrophobic isoleucine-containing ones. This new SELR also presented a dual SA similar to the previous one. Thus, the ELR domain causes the molecule to undergo a rapid phase transition above the transition temperature. The effect of the SLR domain is then observed because of the slow formation of beta sheets, which are stabilized by the formation of hydrogen bonds. Thus, taking advantage of the two forces synergistically, SA leads to the formation of stable and biocompatible porous hydrogels. This study determined that consistent hydrogels can only be formed when silk motifs are included in the sequence of biopolymers. In contrast, homotypic coacervates are formed when only the ELR domain is present. These authors studied the SA and formation of hydrogels with a microscope to see how they evolve over time, verifying that the structure formed by the SELR shows a change in pore size over time that tends to reach its most stable state. Finally, 3-D encapsulation of bone marrow-derived human mesenchymal stem cells (hMSCs) inside hydrogels was carried out, and it was found that cells seeded within the hydrogel could be isolated as clusters of cells or individual cells, because cells adhere to the walls of the pores.

These results support the use of these hydrogels to study cell behavior under controlled conditions.

Along similar lines, Willems et al.[107] explored the impact that the length of each block in diblock silk–elastin copolymers has on the formation of fibrils, bearing in mind that many silk-like polymers assemble into fibrils. These block copolymers comprise an elastin-like domain (ELR) containing the pentapeptide repetition $(GSGVP)_m$ and a silk-like domain (SLR) containing the octamer repetition $(GAGAGAGQ)_n$. Different polypeptides were designed to study the effect of length, combining the ELR block with lengths of $m = 40$, 60, and 80 with the SLR block with lengths of $n = 6$, 10, and 14. The aim was to identify optimal block lengths for a templated SA. The results showed that, for the silk–elastin $(ELR)_m$–$(SLR)_n$ diblock, no fibers were formed when $m = 80$ and $n = 6$. However, for the rest of the possibilities ($m = 80$ and $n = 10$ and 14), fibrils were always formed although in a concentration-dependent manner, with SA into very long fibrils at a high concentration and into short fibrils at a low concentration. When the SLR domain is $n = 14$, no differences in the length of the fibrils were observed for all lengths of the ELR domain ($m = 40$, 60, and 80). However, for diblocks with an SLR domain length of

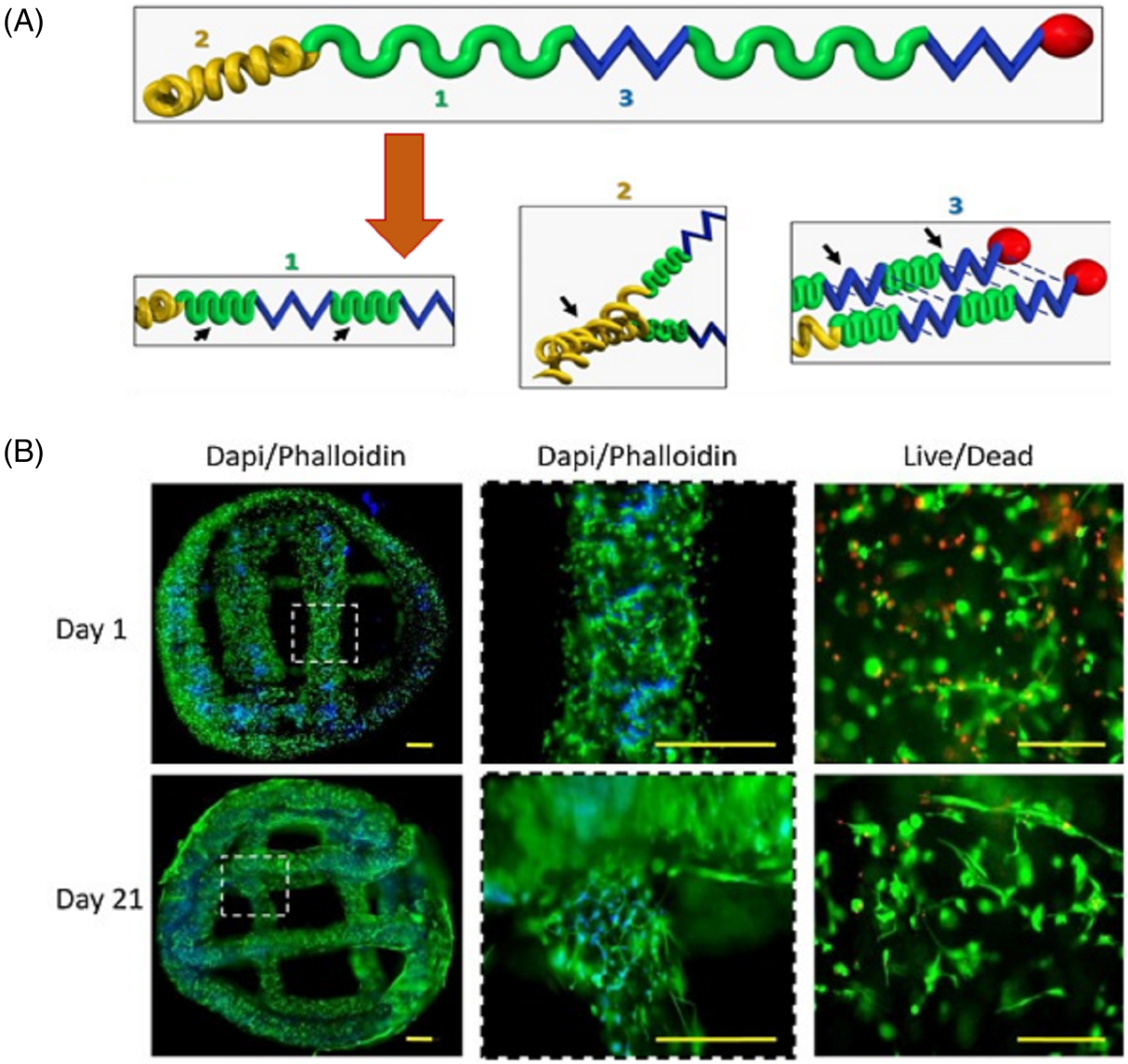

FIGURE 2 (A) Graphical scheme of the different interactions present in the peptide blocks that make up the new elastin-like recombinamer (ELR) bioink. When the polymer is below its transition temperature (T_t) presents a disordered state into random coils. However, when enough energy is provided and the temperature is above the transition temperature (T_t), a mechanism consisting of three-stage gelation is observed. First, reorganization of the elastin blocks, leading to α-helix structures **(1)** is detected. Then, dimerization of the α-helix domains into coiled coil motifs through zipper domains **(2)** is inspected. These two interactions provide structural integrity throughout the printing process, preventing the scaffold from collapsing. Finally, interaction of the silk domains to induce β-sheet secondary structures **(3)** is developed. This interaction provides stiffness to the printed structures, avoiding their disintegration and maintaining their printed shape. (B) Fluorescence microscope images of live/dead and dapi/phalloidin staining of the ELR bioink scaffolds loaded with HFF-1 from Day 1 to Day 21. Scale bar for dapi/phalloidin: 500 μm; for live/dead: 200 μm. Adapted with permission from Salinas-Fernández et al.[108]

$n = 10$, it was observed that the fibrils were shorter as the ELR domain length increased from $m = 40$ to $m = 80$ for the same concentration. As such, the elastin blocks are able to modulate assembly of the silk blocks in such a way that longer elastin blocks lead to shorter fibrils at low polypeptide concentrations. This work therefore demonstrates that a minimum length of the SLR domain is needed to ensure that fibrils can be formed at high polypeptide concentrations, with the $(ELR)_{80}$–$(SLR)_{10}$ copolymer appearing to be the optimal choice for template-induced fibril formation for use in tissue engineering.

More recently, Salinas-Fernández et al.[108] went one step further and developed a new more complex smart material that allows the sequential gelling of a hydrogel, thus obtaining a highly desirable candidate to form biocompatible printable bioinks. As was later demonstrated when using this material to print structures, HFF-1 cells were able to proliferate within them (Figure 2). This new biomaterial was obtained by combining blocks that include the elastin domain (ELR) and the silk domain (SLR) with another block that consist of the Leucine zipper domain (ZR). The difficulty in designing the molecular structure that an ELR must have to behave like an ink lies in inducing the properties of printability and stability during SA in a supramolecular hydrogel. For this, a complex sol–gel transition of the ELR was induced by three consecutive gelling stages: Firstly, the elastin domain (EL), $[(VPGVG)_2\text{-}(VPGEG)\text{-}(VPGVG)_2]_{10}[VGIPG]_{60}$, induces a thermally induced primary rapid gelation based on hydrophobic interactions. Secondly, the leucine zipper domain (ZR), VGGGG GKENQIAIRASFLEKENSALRQEVADLRKELGKCKNILAKYEAGGGGG, carries out a second stabilization by forming amphiphilic alpha-helical structures whose hydrophobic interaction forces them to associate in a spiral pattern. And finally, the silk domain of (SLR), $(GAGAGS)_5$, favors hardening of the structure over time via the formation of beta sheets. As such, this work presented a novel bioink that undergoes rapid SA, thus allowing printability in 3-D devices and, in turn, remains stable over time due to hardening of the silk.

Amyloids

The formation of amyloid fibers is a crucial aspect in the field of IDPs, because predominantly disordered sequences are involved in the formation of prions/amyloids that lead to neurodegenerative disorders such as Alzheimer's or other different diseases.

Rauscher et al.[55] in their work systematically analyzed the aggregation capacity of a wide variety of elastomeric proteins (including elastin), taking into account the impact of the total glycine and proline composition of the peptide chain on these aggregated states. Rauscher et al. demonstrated that there is an approximate threshold value for the total amount of proline and glycine above that amyloid formation is prevented and, therefore, elastomeric properties are observed. In this way, when the total content P + G is between 0.5 and 0.6, the elastic behavior is observed. In this region, the P:G ratio is very diverse with proportions varying from 1:2 to 1:4 (in human elastin or spider silk) to 4:1 (eggshell). On the contrary, in amyloid formation, the content of total P + G is lower than 0.3 (Figure 3). With 60% glycine and 20% proline, the pentapeptide building block of ELRs represents an almost perfect elastomeric protein; however, this feature

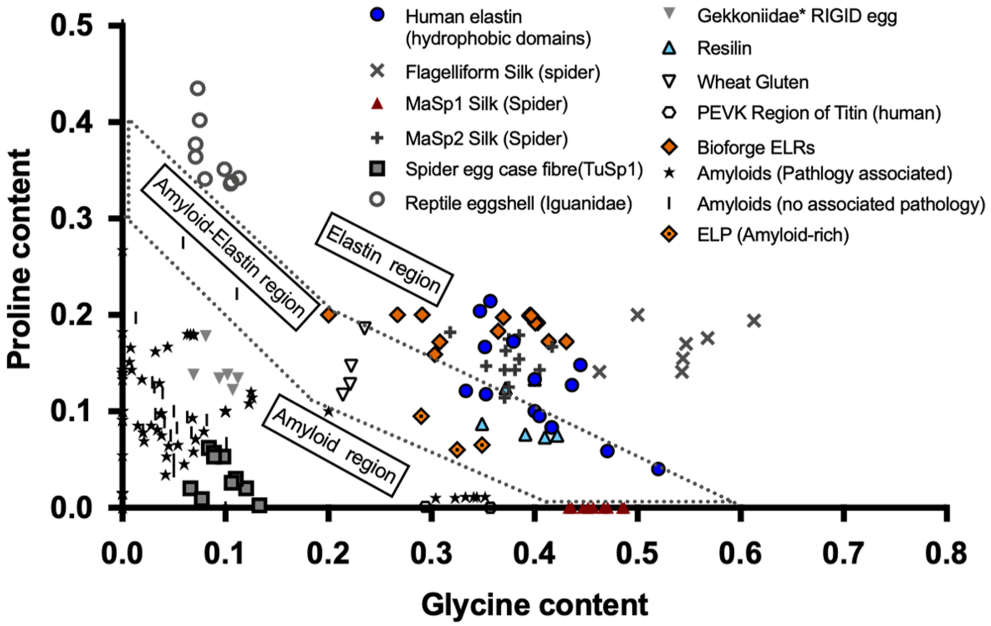

FIGURE 3 Proline and glycine composition of elastomeric and amyloidogenic sequences for different polypeptides including Bioforge elastin-like recombinamers (ELRs) (with permision from Mbundi et al.[109] original one from Rauscher et al.[55]). There is an area in the graph (dotted lines) where the coexistence of both elastomeric and amyloidogenic properties occurs. On the bottom left area are the amyloidogenic sequences whereas on the top right area are the elastomeric sequences. It is observed that many of the elastin domains are composed of a content of 0.4 of G and 0.15 of P. On the contrary, in amyloid formation, the content of G is approximately 0.1, whereas the content of P is 0.15. Therefore, every two glycine residues have the effect of a single proline at this threshold (limit between elastomeric and amyloidogenic), thus highlighting the role of proline as a fundamental component in the establishment of elastomeric properties

does not completely exclude ELRs from being capable of forming amyloids. The modification of the simple sequences of the ELRs and the inclusion of guest residues such as glutamine or asparagine, frequently present in prions, can serve as a model to study how the amino acid sequence can affect the formation of amyloids in an artificial protein polymer. Furthermore, if the third residue of the consensus pentapeptide (glycine, G) is replaced by alanine (A), a change in the elastic properties of ELRs towards plastic deformation (amyloid) can be observed. This can be explained due to the fact that when the dipeptide PG is substituted by PA, a change occurs from type II β-turn to type I, thus varying both the T_t of the polymer and its elastic–plastic properties.

One of the studies that deals with amyloid formation was published by del Mercato et al.,[110] who carried out the structural characterization of amyloid-type fibrils self-assembled from synthetic polypentapeptides, poly (VGGLG), whose monomeric sequence is a repetitive building block of simple and recurrent elastin. This polymer adopts a cross-beta sheet type structure that favors assembly into amyloid-type fibrils. The elastic properties of the fibrils obtained were analyzed to determine the supramolecular assembly and compared with the elasticity of natural elastin, finding that the Young's modulus of the fibrils was higher than that of natural elastin.

Finally, Sharpe et al.[111] developed autofluorescent fibrils using the octapeptide (GVGVAGVG). This sequence (GVA) is derived from the hydrophobic fragment repeat, $(VPGVG)_n$, of human elastin but with a single substitution of the amino acid proline for the amino acid alanine. This is the shortest and best-defined peptide reported to date that exhibits intrinsic fluorescence in the absence of a discrete fluorophore. Such fluorescent fibrils have a predominant beta-sheet conformation, which is probably assembled in an amyloid-like cross-beta structure. The importance of this study can be attributed to the potential utility of fluorescent peptide assemblies as building blocks for new biomaterials.

5.3 | Chemically cross-linked systems with controllable order–disorder balance

Protein-based hydrogels serve as attractive in vitro biomimetic scaffolds for 3-D cell encapsulation, tissue engineering, or drug-delivery applications. The highly hydrated network of hydrogels makes them analogous to the environment in which cells are found in native tissues. To that end, the process of hydrogel formation must be mild and cell compatible, which is easier to achieve in physical hydrogels than in covalently cross-linked hydrogels, which require the use of a cross-linker that may be cytotoxic or lead to undesired reactions or effects. However, some specific applications, such as living-cell encapsulation for both in vitro and in vivo models to study cell–matrix interactions, may require the use of chemical hydrogels because they possess greater stability and improved mechanical properties compared with physical hydrogels. Thus, in this case, cytocompatible cross-linkers are required to perform the chemical cross-linking in order to afford biocompatible hydrogels.

In the search for suitable cross-linkers, only a limited number have been found to be biocompatible. Thus, Heilshorn et al. introduced a new and reliable cytocompatible cross-linker known tetrakis(hydroxymethyl)phosphonium chloride (THPC),[112] which is capable of reacting with primary and secondary amines in aqueous solution in a manner that allows 3-D cells encapsulation in protein-based hydrogels by reacting with the amine groups of various amino acids (Table 1). This new and inexpensive cross-linker was utilized to tune the hydrogel gelation time (6.7 ± 0.2 to 27 ± 1.2 min) and mechanical properties (storage moduli ∼250 Pa to ∼2200 Pa) of hydrogels based on ELRs that exhibited cytocompatibility for 3-D encapsulation of two cell types, namely, embryonic stem cells and neuronal cells.

An innovative one-pot method for fabrication of 3-D "bead-string" microstructured ELR hydrogels with the simultaneous THPC chemical cross-linking and physical SA has been developed by Wang et al.[113] The gel microstructure as well as the size and density of polymer-rich coacervates present in the material structure was controlled by tuning the cross-linker ratio and covalent cross-linking reaction time before the thermally triggered assembly. A sparsely cross-linked network allows the ELR to have greater chain mobility, thereby resulting in a physical phase transition into larger beads. As the cross-linking density increases, the ELR chain mobility is more restricted, and smaller beads are obtained as a result of a more delimited chain SA process. These sophisticated bead-string microstructured hydrogels were exploited for dual encapsulation of a hydrophilic drug, namely rhodamine-B isothiocyanate-dextran, and a hydrophobic drug, namely, coumarin-6. The hydrophobic drug is preferentially localized in the thermal aggregates, whereas the hydrophilic drug is predominantly dispersed in the polymer-lean phase of the hydrogel. The hydrophilic drug was delivered with faster kinetics than the hydrophobic drug, which is located in a polymer-rich phase with much smaller mesh size. These different release rates for encapsulated drugs, controlled by the self-assembled bead-string microstructure, make these gels promising for biomedical applications, including drug delivery.

The development of hydrogels as tunable engineered matrices allows studies of the cellular response to specific properties of ECM analogs. In fact, a fundamental aspect in tissue engineering is the study of the effect of microenvironment on cell differentiation. Thus, a new study devoted to analyze the effect of hydrogel cross-linking density on cardiomyocyte (CM) differentiation in murine embryoid bodies (EB) was performed with ELRs, which are attractive due to their ability to mimic cardiac tissue properties, such as modulus or resilience.[114] The ELR hydrogels were formed with THPC as cross-linker, and hydrogel cross-linking density was tuned by varying the cross-linker to protein stoichiometry (0.5:1, 0.75:1, and 1:1). CM differentiation was accelerated in hydrogels with a lower cross-linking density (0.5:1), which provided a more supportive environment for cellular growth, proliferation, and cell-dictated ECM remodeling than their more densely cross-linked counterparts.

In a related study, in order to determine the role of a bioactive adhesive domain at the hydrogel in cardiac cell differentiation, an ELR

TABLE 1 Different approaches for obtaining chemical hydrogels, control of their biochemical and physical properties for biomedical applications

Hydrogel formation	ELR funtional domain/sequence	Physical/biochemical properties	Application	Ref.
THPC/ physical assembly	• $[(VPGIG)_2VPGKG(VPGIG)_2]_3$	• Gelation time and mechanical properties tunning • 3-D "bead-string" microstructure	• Controlled drug delivery	Chung et al.[112] Wang et al.[113]
THPC cross-linking	• $[[(VPGIG)_2VPGKG(VPGIG)_2]_3]_4$	• Cross-linking density • THPC/protein ratio	• Cardiomyocyte differentiation	Chung et al.[114]
THPC cross-linking	• $(GGK)_3(VPGIG)_{25}$GGRSGRGDSPALQGG $(GGK)_3(VPGIG)_{25}$GGVDGRGDSPAELGG	• Soft hydrogels • RGD adhesion domain role	• Cardiac cell differentiation	Kambe et al.[115]
SPAAC "Click chemistry"	• $\{[(VPGIG)_2(VPGKG)(VPGIG)_2]_2$-AVTGRGDSPASS-$[(VPGIG)_2(VPGKG)(VPGIG)_2]_2]\}_6$ • $[VPGKG(VPGVG)_5]_{24}V$	• Temperature • Concentration	• Heart disease	Previous studies[116–118]
SPAAC Staudinger "Click Chemistry"	• $[[(VPGIG)_2VPGKG(VPGIG)_2]_3]_4$ • TVYAVTGRGDSPASSAA	• BCN-ELR ratio • Concentration	• hMSCs, HUVEC, and mNPCs encapsulation	Madl et al.[119]
SpyTag/ SpyCatcher "Isopeptide bond"	• SpyTag (AHIVMVDAYKPTK) • RGD/MMP-1	• β-Sandwich structure • Introduction of mCherry • Introduction leukemia inhibitory factor	• Mouse 3T3 fibroblast encapsulation • LIF-Spy network for 3-D stem cell culture	Sun et al.[120] Li et al.[121]
Disulfide bridges	$[(VPGAG)_{14}(VPGVG)(VPGCG)]$	• Reversible hydrogels • Mild oxidative conditions	• Injectable hydrogels • Intratumoral infusion in nude mice bearing FaDu tumor	Asai et al.[122]
MCPs CCPs THPC	• HEDGHWDGSEHGY: Zn^{2+} binding domain • GKG: Covalent cross-linking domain	• Strong, tough, and stretchable hydrogels	• Self-adhesive hydrogels	Gonzalez et al.[123]

Abbreviations: BCN, bicyclo[6.1.0]nonyne; CCPs, covalent cross-linking sites; ELR, elastin-like recombinamer; hMSCs, human mesenchymal stem cells; GKG, glycine-lysine-glycine; HUVEC, human umbilical vein endothelial cells (HUVECs); LIF, leukemia inhibitory factor; MCPs, metal cross-linkable domains; mNPCs, murine neural progenitor cells; RGD, arginine-glycine-aspartic acid; SPAAC, strain-promoted azide-alkyne cycloaddition; THPC, tetrakis(hydroxymethyl)phosphonium chloride.

containing an arginine-glycine-aspartic acid (RGD) adhesion sequence (ELR-RGD) was developed to subsequently obtain chemical hydrogels, covalently cross-linked with THPC. These soft ELR-RGD hydrogels, with an elasticity (0.3 kPa) similar to that of embryonic cardiac tissue, were studied in cardiac differentiation of induced pluripotent stem cells (iPSC).[115] The presence of an RGD motif in the hydrogel seems to influence the integrin-β1-derived signaling pathways in iPSCs to stimulate their differentiation. Thus, iPSCs were cultured on the hydrogels, and cardiac differentiation was induced using Ca-rich medium and treatment with TSA, thus resulting in ELR-RGD gels with a four times higher *TnT2* (encoding a contractile protein) expression than for the control gels lacking the adhesive sequence.

Many chemical hydrogels used as 3-D scaffolds for cell culture and transplantation present the limitation of the use of cross-linking agents that can also react with functional groups present on the cell surface and co-delivered biological factors. Bio-orthogonal chemistries that do not cross-react with functional groups found in biology, thus preventing undesirable side reactions, have progressed since their initial introduction by Prescher and Bertozzi and Sletten and Bertozzi two decades ago.[124,125] This bio-orthogonal chemistry includes copper(I)-catalyzed azide-alkyne cycloaddition (CuAAC),[126,127] strain-promoted azide-alkyne cycloaddition (SPAAC),[128] Staudinger ligation,[129] tetrazine ligation,[130] and traditional Diels–Alder reactions.[131]

A novel and biocompatible ELR chemical hydrogel based on a two-component system comprising a structural ELR (ELR-VKV) and an ELR containing an RGD cell-adhesion sequence (ELR-RGD), in a process avoiding the use of a catalyst, using bio-orthogonal chemistry and with the biopolymer chains themselves acting as cross-linkers, has been developed by González de Torre et al.[116] Both these ELRs were chemically modified to bear the reactive groups, azide, and bicyclo [6.1.0]nonyne (BCN), involved in a SPAAC "click" chemical reaction. Thus, the ELRs' hydrogel was formed under physiological conditions in an atom-economy process that does not release any by-product. Varied microstructures leading to tunable physical and mechanical properties were obtained when the hydrogels were obtained at different concentrations and at different temperatures. Poroelasticity and intrinsic viscoelasticity dominate on a frequency scale, as

demonstrated by rheological measurements. These biocompatible hydrogels have been widely used in biomedical applications such as heart diseases.[117,118]

Two new ELR-based chemical hydrogels produced either by SPAAC or by a Staudinger ligation reaction have been developed, with tunable mechanical and biochemical properties.[119] Their behavior in gelation determined that whereas formulations of SPAAC-cross-linked materials completed gelation in a matter of minutes (reaching their plateau storage moduli within a few minutes), those ELRs cross-linked using Staudinger ligation (triarylphosphines mediated) took much longer to gel, with complete gelation observed after 1 h. In addition, SPAAC-ELP hydrogels exhibited independent tuning of stiffness and cell adhesion upon varying the molar ratio of BCN groups per ELR or the polymer content of the hydrogel. These elastic materials exhibited a higher cross-linking density as the BCN:ELR molar ratio increased (4:1–5:1), thus resulting in higher storage moduli. The same trend was observed when the polymer content of the gels was increased at a fixed BCN:ELR ratio. Because rapid gelation kinetics are ideal for cell encapsulation, SPAAC hydrogels were used to support the encapsulation of hMSCs, human umbilical vein endothelial cells (HUVECs), and murine neural progenitor cells (mNPCs). These SPAAC hydrogels showed acute viability and longer term phenotypic maintenance for all cell types tested. Furthermore, hydrogels containing the cell-adhesive RGD sequence supported enhanced viability and spreading of hMSCs compared with those control hydrogels containing a non-adhesive, scrambled RDG sequence. Moreover, increased spreading was observed as hydrogel stiffness decreased, probably due to an inability of MSCs to cluster the ligands and allow stable adhesion in overly stiff hydrogels.

A second approach to obtain hydrogels that cross-link without requiring any chemical reagent is based on the design of two ELRs capable of bonding via a specific isopeptide link formed between Asp-117 of SpyTag-ELR and Lys-31 of SpyCatcher-ELR and under physiological conditions.[120] The resulting "network of Spies" shows a compact β-sandwich structure in which SpyCatcher interacts with one side of SpyTag and strong hydrophobic interactions between the side chains as well as extensive hydrogen bonding network are also produced.[121] Because of the recombinant nature of the starting biopolymers, the spy network also includes cell-adhesion ligands and matrix metalloproteinase-1 cleavage sites. This matrix was evaluated for mouse 3T3 fibroblast encapsulation, with a high cell viability (95%) being observed after 24 h. Moreover, cells exhibited elongated morphologies, indicative of cell adhesion and matrix remodeling enabled by the inclusion of RGD and MMP-1 sites in the network. To complete the study, full-length globular proteins, such as mCherry or leukemia inhibitory factor (LIF), were included in the ELR design and integrated covalently into the protein network, where they folded correctly. Indeed, the LIF-modified Spy network supported 3-D stem cell culture with maintenance of stem cell pluripotency, thus making Spy networks particularly promising platforms for the study of cell–matrix interactions.

Reversible thermally responsive ELR-based chemical hydrogels have been developed by Asai et al. in a process that proceeds with rapid gelation under physiological and mild oxidative conditions.[122] This reversible sol–gel transition occurs due to the formation of intermolecular disulfide bridges that are easily broken under reducing conditions. These reversible hydrogels offer useful features that are intermediate between covalent cross-linked gels and coacervates, such as rates of degradation and clearance. ELRs incorporating periodic cysteine residues (cELRs) were designed and the gelation process triggered by addition of hydrogen peroxide (0.3 wt%). The rheological properties of these cELRs confirmed their rapid gelation, at concentrations as low as 2.5 wt%, under mild oxidative conditions. cELR hydrogels are useful injectable biomaterials in vivo, as confirmed by a study of intratumoral infusion in nude mice bearing FaDu tumor xenografts using [^{125}I]-labeled ELRs. cELR hydrogels showed prolonged intratumoral retention, a homogeneous distribution across the entire tumor, and fast enough gelation (<2.5 min) to be useful in drug delivery and regenerative medicine applications.

Strong and self-adhesive hydrogels have been obtained from genetically engineered unstructured proteins by covalent and reversible cross-linking.[123] To that end, two new recombinamers, one comprising ELR domains interspersed with metal cross-linkable domains (MCPs) and the other comprising ELR domains interspersed with covalent cross-linking sites (CCPs), were designed. The unstructured nature of the proteins was studied using force-extension curves for the single molecules and also confirmed by CD spectroscopy in which CCPs and MCPs showed characteristics of disordered polypeptides. The MCP chosen contains a zinc-binding motif with the amino acid sequence HEDGHWDGSEHGY, and the CCP contains the tripeptide GKG (glycine-lysine-glycine) in which the lysine (K) residue serves as a CCP. The gene assembly method enabled to precisely control the composition of the ELRs and their length, the density of each domain, and the molecular weight of the biopolymers and also allowed control of the mechanical properties of the hydrogels obtained. Mixtures of both ELRs (CCPs and MCPs) formed hydrogels upon covalent cross-linking with THPC, with the cross-linker reacting with lysines from the GKG domain. A high water content (70–75 wt%) and transparent appearance were achieved for these chemical hydrogels. Subsequent immersion in zinc sulfate solutions of different concentrations caused the MCPs to cross-link via metal coordination. The water content of the resulting hydrogels ranged from 32 to 96 wt%, depending on the Zn^{2+} concentration in the solutions, and those networks with a $ZnSO_4$ concentration of 2.0×10^{-3} M or higher appeared opaque as the kosmotropic salt lowered the ELR transition temperature to a value below ambient. As such, these hydrophobic interactions in the hydrogel enhanced their mechanical properties and achieved improvements in stiffness, stretchability, and strength. These unstructured protein networks also demonstrated self-adhesive behavior in Zn^{2+} solutions as a result of metal coordination and the hydrophobic interactions of the network across the material interface. These strong, tough, and stretchable materials may provide a robust scaffold for use in biomedical applications such as tissue engineering.

6 | ORDER–DISORDER AND BIOMINERALIZATION

Biomineralization is a process in which living organisms form mineral-like materials under strict biological control. This process involves a controlled deposition of calcium phosphate minerals into an organic matrix, which is responsible for the structure and subsequent function of mineralized tissues.[132] The organic matrix nucleates and directs the hierarchical growth and morphogenesis of mineralized tissue, with the specific properties of this matrix, such as charge, conformation, and supramolecular assembly, playing key roles in the biomineralization process.[133]

Intrafibrillar mineralization of type I collagen fibril, in which the collagen fibrils serve as an organic template that directs both the infiltration and orientation of hydroxyapatite, is one of the most important biomineralization processes.[134–136] The structure of type I collagen consists of three left-handed polyproline peptide chains intertwined in a right-handed manner, with the triple-helical collagen molecules packed in a quasi-hexagonal mode.[137] A collagen mineralization bioinspired approach was studied by Li et al.,[62] who performed intrafibrillar mineralization of ELR fibrils to afford a stable inorganic–organic nanocomposite that mimics the nanostructure of bone. ELRs, as thermally responsive molecules, remain in an unfolded state below T_t and, above T_t, initially self-assemble into a quite dynamic β-spiral by recurrent formation of type II β-turns. These poly(VPGXG) molecules further associate into multistranded twisted filaments. Before biomimetic mineralization, the fibrils were fixed by covalent cross-linking with isocyanate. After mineralization for 7 days, calcium phosphate precursors infiltrated into the interstitial spaces of the ELR fibrils and formed needle-like hydroxyapatite (HAP) nanocrystals. Much denser sponges were formed when using ELRs with bioactive sequences that disturbed the initial β-spiral formation, thus suggesting that the fibrils coalesced before mineralization. These results indicate that the regular self-assembled structure of poly(VPGXG), rather than bioactive sequences such as SNA15 or electrostatic interactions in the recombinamer composition, play a key role in intrafibrillar mineralization.

A new class of hybrid nanocomposites with controlled morphologies has been obtained from insoluble organic matrices as porous hydrogels of ELRs, which have been mineralized through a biomimetic polymer-induced liquid-precursor (PILP) process in a bottom-up method. The original microstructure of the hydrogel was used as template in a calcium phosphate mineralization process in which the minerals, or hydroxyapatite nanocrystals, were infiltrated into the hydrogel frameworks, thereby preserving their microporous structure.[138]

The amphiphilic triblock ELRs designed for this purpose comprised a hydrophobic block enriched in alanine surrounded by two hydrophilic blocks bearing the statherin-derived analog DDDEEKFLRRIGRFG (SNA15). The thermoresponsive and microporous hydrogels formed by covalent cross-linking using carbodiimide chemistry were transparent at 4°C and became opaque at 37°C, thus

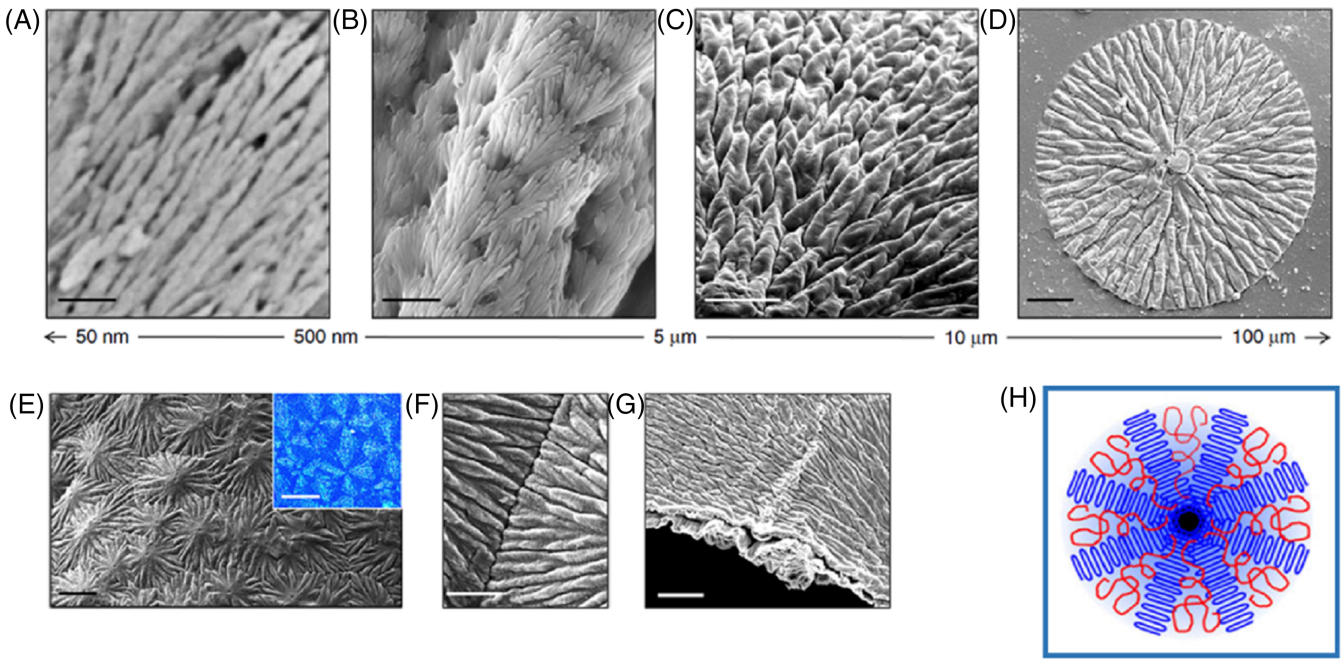

FIGURE 4 Elastin-like recombinamer (ELR)-mediated mineralization process resulted in the growth of distinctive hierarchically ordered mineralized structures. (A–D) Scanning electron microscopy (SEM) images of an ELR membrane after mineralization, top part, showing the hierarchical organization of the mineralized structures: (A) aligned fluorapatite nanocrystals that are (B,C) grouped into prism-like microstructures that further (D) grow into macroscopic circular structures. (E,F) Hierarchical structures meet each other and (G) finally can mineralize completely thin membranes. (H) Picture of the ELR with disordered random coil, red, and ordered β-sheet structure, blue. Scale bars: (A) 200 nm; (B) 1 μm; (C) 10 μm; (D) 20 μm; (E) 30 μm; (E [inset]) 20 μm; (F) 5 μm; (G) 20 μm. Adapted with permission from Elsharkawy et al.[140]

indicating that a phase transition occurred. Microphase separation (microdomains in tens of nanometers) between hydrophobic and hydrophilic moieties is responsible for nanopore and/or nanochannel formation within the hydrogel framework, thus serving as compartments for mineral deposition. Mineralization was conducted using a PILP process, a biomimetic mineralization system in which anionic polyaspartic acids mimic the role of acidic proteins in biominerals, thus forming a liquid-like amorphous calcium phosphate (ACP) precursor complex.[139] After mineralization for 28 days, a mineral density of up to 1.9 g/cm,[3] which is comparable with that for natural bone and dentin, was obtained. In the dry state, the elastic modulus and hardness values of the mineralized hydrogels were lower but still of the same order of magnitude as those for natural hard tissues. The results indicated that the recombinant nature of ELRs allows them to be especially promising candidates for controlling the morphologies of ELRs matrices as they can be used to construct diverse hybrid nanocomposites with optimized mechanical and biological properties for bone defect treatments. Moreover, the ability to tune the chemical and physical properties of ELR hydrogels could help to elucidate the mechanisms involved in the mineralization process in living organisms.

A protein-mediated mineralization process was studied by Elsharkawy et al.[140] in order to take advantage of the disorder–order interplay of ELRs that are able to arrange organic–inorganic interactions into hierarchically ordered mineralized structures. Dynamic organic matrices for biomineralization were designed based on a recombinant molecule that comprises both intrinsically disordered regions and negatively charged domains. Thus, an ELR was designed to comprise a main hydrophobic framework (VPGIG), a positively charged segment (VPGKG) with the amino acid lysine (K) for ELR cross-linking, and the highly acidic statherin-derived analog DDDEEKFLRRIGRFG (SNA15), which is negatively charged at physiological pH. This SNA15 segment, which comprises 15 amino acids and is situated at the N-terminus, is also known to promote mineralization.[141,142] Once the ELRs had been cross-linked with hexamethylene diisocyanate (HDI), they self-assembled into a dense network of β-amyloid-like fibrils together with homogenously distributed 3-D ELR spherulites due to the presence of VPGXG tropoelatin motifs. Mineralization resulted in the growth of distinctive hierarchically ordered mineralized structures that appeared to emanate from the ELR spherulites. Moreover, membranes made from the statherin-derived ELR presented a higher number of mineralized structures, thus suggesting that nucleation increases with the number of acidic amino acids present within the ELR molecule. The mineralized structures exhibited elongated apatite nanocrystals that were aligned and organized into microscopic prisms, which grow radially into circular structures that come together to fill macroscopic areas (Figure 4). The material showed high stiffness, hardness, and acid resistance and could be fabricated as fully mineralized membranes or coatings over uneven surfaces, including native tissues. Moreover, the simplicity and versatility of this mineralization platform allow it to be used to address the regenerative challenges of mineralized tissues and provide insights into the role of molecular disorder in human physiology and pathology.

Arterial calcification involves deposition of calcium phosphate (Ca−P) minerals on the intimal and medial layer of the arteries in the ECM. Intimal calcification is commonly associated with atherosclerosis, with minerals being predominantly deposited on collagen fibers. Conversely, medial calcification is associated with aging, chronic kidney disease (CKD), and type II diabetes,[143,144] with mineral deposition occurring predominantly on elastin-rich elastic laminae. Investigation of the unknown mechanism of mineral formation on these elastin layers was the reason for the research carried out by Gourgas et al.[145] The in vitro model for medial arterial calcification designed by these authors consisted of ELR hydrogels cross-linked with genipin and subsequent SA induced by adding salt and heating. An initial mineralization procedure was carried out in simulated body fluid (SBF, 1.5×) at physiological pH and temperature. As in in vivo mineralization, Ca^{2+} is initially adsorbed because elastin fibers and filaments are prone to mineralization. ACP and octacalcium phosphate (OCP) are formed initially, evolving to more crystalline apatite phases, thus agreeing with previous observations in a mouse model of medial calcification,[146] thereby suggesting that this simple system reproduces some of the key in vivo findings. A subsequent study was performed to try to enhance the kinetics of mineral deposition in this model.[145] Thus, highly concentrated SBF solutions were employed in the mineralization process, and the effect on mineral formation and phase transformation on ELP membranes immersed in high concentration SBF was studied. Evolution of the mineral phase was found to be strongly affected, with the mineral being less prevalent and transforming very quickly into apatite phases. The final apatite phase was less crystalline and Ca-deficient, and the mineral deposits became more disordered and densely packed as SBF concentration increased. This mineralization model is more appropriate to study medial calcification in patients with life-threatening diseases such as CKD, whereas the study of mineralization using low concentrated SBF is better suited to the study of medial calcification associated with the loss of calcification inhibitors.

7 | MULTIVALENT COATINGS AND FILMS BASED ON IDPS

The development of new systems for spatial control of cell adhesion, for biomaterial-associated infection (BAI) treatment or, in general, for enhancing tissue material interactions, based on the ELR coating of material surfaces using different techniques is reviewed in this section.

The ability to control the arrangement of cells on material surfaces enables fundamental investigations in cell biology and tissue engineering, such as those devoted to modulation of cell–cell interactions, directed stem cell phenotype studies or 2-D cell migration studies.[147,148] On the other hand, the increasing use of temporary or permanent biomedical devices brings with it difficult-to-treat problems, such as the risk of bacterial infections due to the formation of an adherent bacterial biofilm on the surface of the biomaterials (increasing the appearance of multidrug resistant bacteria), thereby often resulting in extensive use of antibiotics and even revisional

surgery.[149] Some strategies involving the use of bactericidal and antifouling surfaces to prevent bacterial adhesion and inhibit biofilm formation have been reviewed.[150,151] In this regard, the use of nanocoatings based on AMPs appears to be a promising choice to prevent bacterial infections.

Well-defined and stable cellular patterns have been obtained on gold micropatterned silicon substrates generated by photolithography.[152] This strategy takes advantage of the different orientation of the biopolymer when adsorbed on either gold or silicon regions of the patterned surface. Immobilization of peptides on gold regions via C-terminal end thiol groups from RGD-ELP-Cys biopolymers carrying a cysteine-rich binding domain enablese their C-terminal chemisorption (grafting) onto gold regions as a result of a redox reaction, thus leading to a uniform molecular orientation whereby available N-terminal GRGDS cell-binding domains are accessible for cell adhesion. In contrast, RGD-ELP-Cys adsorbed on silicon oxide regions hinders the accessibility of cell-binding domains due to their random orientation. This dissimilar accessibility of cell-binding domains has been evidenced by enhanced cell adhesion, and spreading, on the coated gold regions and by minimal cell adhesion within silicon oxide regions. The cells confined within the polypeptide-modified gold regions were viable and maintained pattern integrity for up to 8 weeks, thus suggesting long-term maintenance of patterned cells. In this study, ELRs were acting with a double purpose, namely, as a biolinker for both active peptide domains and a modulator of cell response as a result of their spatial arrangement.

Following the same strategy of including a cysteine-rich domain at the end of the biopolymer, which allows covalent binding to a gold surface, Flora et al.[153] designed a new and simple system for cell selectivity and spatially controlled cell adhesion. The system includes model gold surfaces grafted with a combination of two ELRs containing cell-adhesion domains such as RGD and REDV in their backbone. To achieve this goal, whole model gold surfaces were initially biofunctionalized with the ELRs including CC-RGD by grafting them to the surface by way of a redox reaction with thiol groups but this time present in the amino terminal cysteine tails of the ELRs. Several strips were then cleaned by laser ablation and grafted with a mixture of two ELRs with complementary bioactivity (25% CC-RGD and 75% CCC-REDV). This ELR ratio was previously optimized in an in-depth adhesion study, which showed that the mixture of 75% ELR-REDV (with a specific adhesive sequence for endothelial cells) and 25% ELR-RGD (a universal cell-adhesion sequence) exhibited a high selectivity for endothelial cells, thereby promoting the strong adhesion thereof. The synergy between these two different bioactivities, which produces an enhanced cell-selectivity effect, was clearly demonstrated.

Spatially controlled cell adhesion was obtained when a co-culture of HUVEC and HFF-1 cells was employed (Figure 5), with a marked increase in the adhesion of endothelial cells on the strips functionalized with 75:25 REDV:RGD and selective adhesion of HFF-1 cells on the other areas functionalized with 100% RGD. This spatial segregation of the co-culture of HUVEC and HFF-1 cells is due to the bioactive epitopes (RGD and REDV) present on the backbone

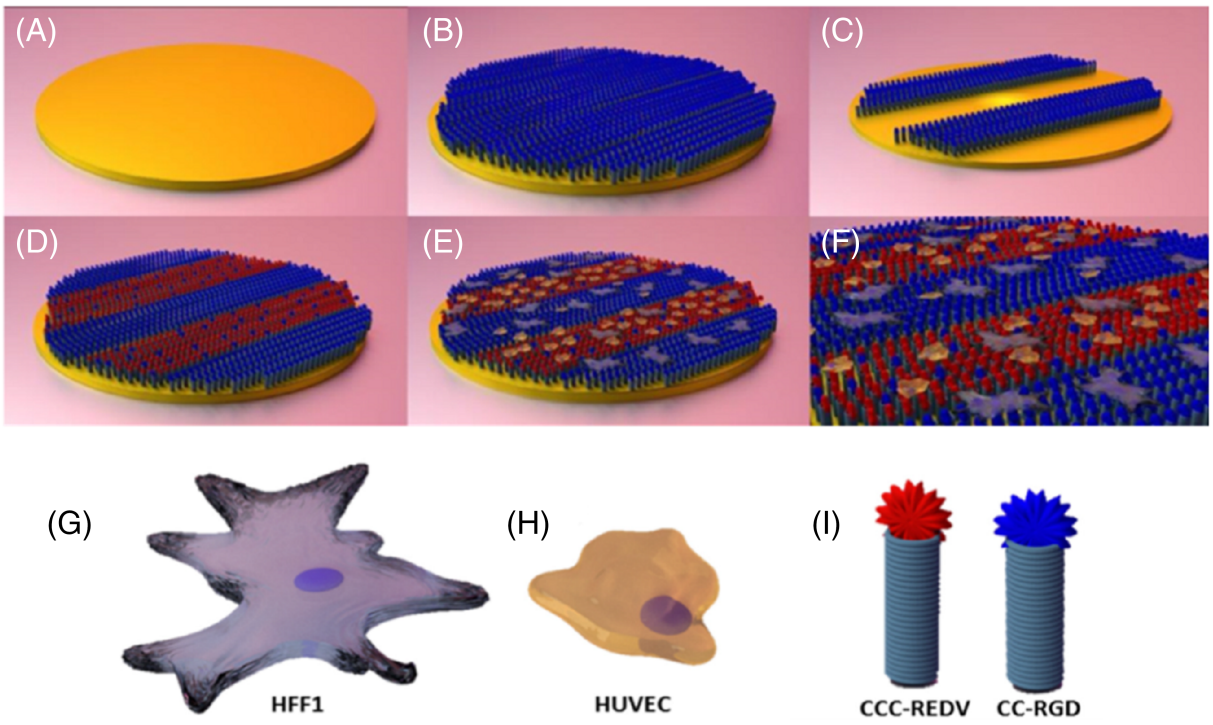

FIGURE 5 Spatially controlled cell adhesion on differently biofunctionalized surfaces. (A) Nonfunctionalized gold surface; (B) gold surface functionalized with CC-RGD; (C) strips cleaned by laser ablation; (D) ablated strips functionalized with 75% CCC-REDV/25% CC-RGD; (E) human umbilical vein endothelial cell (HUVEC) and HFF-1 cells adhesion; (F) magnification of adhered cells. Representation of (G) fibroblast cells (HFF-1), (H) endothelial cells (HUVEC), and (I) CCC-REDV (red color) and CC-RGD (blue color) recombinamer. Adapted with permission from Flora et al.[153]

of the ELRs, because each functionalized surface (including strips) has similar topographic and hydrophobic characteristics, and the mechanical properties are of the same order of magnitude.[154]

An efficient system for spatial control of cell adhesion is valuable for subsequent applications such as drug discovery, biomedical engineering, and intercellular applications, as well as for the study of fundamental cell biology and the production of cell-based biosensors and diagnostic devices.

A new study of the biofunctionalization of titanium bone-implant surfaces was reported by Salvagni et al.,[155] including immobilization on the surface of ELRs combining a bioactive motif for cell adhesion with protein antifouling properties. ELR immobilization was carried out in two different approaches, one of them involving physical RGD-ELR adsorption via electrostatic interactions and the second involving RGD-ELR covalent-grafting using organosilane chemistry and via the amine groups of the lysines present in the ELR (VPGKG domain). The coated titanium surfaces exhibited antifouling properties, with excellent reduction of serum-protein adsorption (9 ng/cm^2) compared with the bare metal surface (310 ng/cm^2). These surfaces also exhibited improved bioactivity and better hMSC adhesion in terms of cell number, cell spreading, and focal point expression.

Ti and its alloys are biocompatible materials but also bioinert, thus leading in some cases to long osseointegration processes, loosening, and inflammation that may eventually result in rejection of the implant.[156–158] No bone-implant contact enhancement was observed when simple RGD was present at the titanium surface, where the nonspecific adsorption of plasma protein probably covered the RGD signals. This novel and simple biomimetic modification delivers a functionalized metallic surface that combines improved bioactive properties with a reduction in nonspecific protein adsorption. Although covalently bonded coatings require a more complex chemistry, they offer the possibility of achieving more robust supports for tethering biomolecules and show higher stability than physisorbed-biopolymer coatings, thus making them promising candidates for long-lasting implants.

With the aim of improving the performance of immunospecific biosensors, and even achieving specific multichannel cell labeling, immunoassay surfaces were biofunctionalized with multiprotein complexes that are able to target and label antigen-presenting eukaryotic cells.[159] Thus, a new ELR was designed to accommodate three different orthogonal conjugation sites and allow one-pot nanoassembly of multiprotein complexes that could be grafted to sensor surfaces in a controlled orientation. The first step in the ELR design provided periodic noncanonical L-azidohomoalanine amino acids, which are able to covalently link single-domain antibodies (SdABs) via click chemistry with the dibenzocyclootine antibody derivative (DBCO)-SdABs, situated at the guest residue position of the elastin domain. Two additional specific tags, namely, ybbR and Sortase A, were included at the ends for ligation to coenzyme A substrates and GGG substrates, respectively, mediated by 4′-phosphopantetheinyl transferase (Sfp) and Sortase A, respectively. A series of immunoassays using mCherry spiked into undiluted human plasma were performed with controlled surfaces modified with multi-SdAbs:ELR complexes and compared with surfaces coated with randomly adsorbed antibodies SdAbs. The multi-SdAbs:ELR complex system exhibited a dose–response, and an improvement in sensitivity of between of 2.3- and 14.3-fold and ~30−40% lower limits of detection were obtained, in comparison with nonspecifically adsorbed antibody systems. Subsequent cytometric labeling and analysis of live eukaryotic cells showed that, when attached in a controlled orientation, multi-antibody ELP complexes specifically bound the m-Cherry-positive cells with enhanced immunospecific binding interactions as a result of multivalency effects.

BAI caused by adherent biofilm formation is usually difficult to treat because the biofilm lowers bacterial susceptibility towards antibiotics, allowing them to outwit the immune system.[160–162] This often results in retrofitted surgery as well as the overuse of antibiotics. One alternative to antibiotics would be to include the use of AMPs. AMPs are small amphiphilic peptides (12−50 amino acids) that are usually positively charged and are able to self-assemble and[163] interact with multiple cellular components of both an infectious agent and a host.

The inherent instability of AMPs prompted research into the development of biomaterial surface coatings to covalently immobilize them in order to increase their stability and minimize their toxicity. In this sense, Atefyekta et al.[164] performed covalent immobilization of AMPs on biomaterial surfaces previously coated with ELRs containing cell-adhesive peptide domains (RGD). ELRs spin-coated onto titanium substrates were further photocross-linked with ultraviolet (UV)-light treatment to form a film in which an AMP known as RRP9W4N (RRPRPRPRPWWWW-NH2) was covalently immobilized onto the ELR surface using carbodiimide coupling chemistry. The resulting implant coating demonstrated a high antimicrobial effect against *Staphylococcus epidermidis*, *Staphylococcus aureus*, and *Pseudomonas aeruginosa*. The chemical stability of the covalently immobilized AMPs in human blood serum, with antibacterial activity up to 24 h, was demonstrated by performing a quartz crystal microbalance with dissipation monitoring (QCM-D) assay and found to be similar to that for AMPs covalently immobilized onto other biomaterial surfaces.[165,166] At the same time, AMP functionalization had no significant effect on the viability, function, and differentiation of human osteosarcoma MG63 cells or hMSCs, as shown by mineralization and alkaline phosphatase tests, did not affect cell-adhesivity, and had no toxic effects on the mammalian cells used. Surface mineralization was not affected by tethering of AMPs, thus maintaining the osseointegrative properties of ELP-coated surfaces over 28 days in vitro, thus meaning that the biomaterial is likely to integrate with the host tissue and making this a promising candidate as an antimicrobial coating for medical devices such as orthopedic implants.

A new bactericidal and antifouling coating to prevent bacterial adhesion and inhibit biofilm formation on biomaterials, in a synergistic manner, was designed using an approach involving the production of multifunctional self-assembled monolayers based on AMPs conjugated to ELRs.[167] The multimodular design of the ELR includes an AMP (GL13K; GKIIKLKASLKLL-NH2), a bioinspired AMP derived from parotid secretory protein (BPIFA2), to be conjugated to a low-fouling ELR based on poly-VPGXG (X = V and K in a 5:1 ratio), as well as the

inclusion of a C-terminal grafting domain for oriented covalent tethering of recombinant polymers onto gold model surfaces. The antibiofilm effect of the AMP against two of the bacterial strains most frequently responsible for indwelling medical device-associated infections, namely, *S. epidermidis* and *S. aureus*, was synergistically enhanced by the antifouling effect of the ELR. The hybrid recombinant coatings were not cytotoxic for human fibroblasts during in vitro culture for periods of up to 7 days, thus showing that the toxic effect is selective for bacteria and does not affect the proliferation of human cells.

The main limitation of AMP-based coatings for clinical materials is their high cost of chemical manufacture, which impedes scale-up.[168] However, the recombinant production of AMPs fused to ELRs enables the efficient production and simple purification of heterologous proteins in a cost-effective scalable process because of their thermosensitive behavior.[169,170] Furthermore, the D- and L-enantiomers of GL13K peptide have been shown to have different SA properties that can compromise their bactericidal activity. Thus, D-GL13K is a protease-resistant peptide that can evade bacterial resistance.[171] Moreover, AMP attachment to the substrate via a spacer enhances their flexibility, exposure, and functional conformation, thereby improving the anti-infective potential and bioactivity of the coatings.[159,172,173]

A more exhaustive study of hybrid antibiofilm coatings based on L- and D-GL13K allowed their incorporation into the ELR backbone by genetic engineering or chemical derivatization, respectively.[65] Thus, L-GL13K-ELR (VCL) was recombinantly produced in *E. coli* BLR (DE3), as described elsewhere,[167] and D-GL13K-ELR (VCD) was produced by chemical modification of lysines to cyclooctyne groups and subsequent strain-promoted azide–alkyne cycloaddition to azide-modified D-GL13K peptides. The resulting hybrid ELRs were subsequently tethered to commercially pure titanium discs using organosilane chemistry. Their biological response was tested in a drip-flow biofilm reactor simulating realistic in vivo environmental dynamic conditions, and an oral microcosm biofilm model collected from cariogenic patients was grown onto the hybrid coatings (VCL and VCD). The presence of the AMPs in the hybrid coatings prevented the formation of a mature biofilm and provided additional bactericidal activity against the bacteria remaining on the surface, with antimicrobial potential after incubation for 6 days. The cytocompatibility of these systems was assessed using mammalian cells present in the oral cavity, namely, primary human gingival fibroblasts, which showed total viability and appropriate proliferation, thus showing that they are safe for dental applications. So, ELRs serve as a functional platform for AMP-tethering, and these ELRs allow proper folding of the AMPs domains that were active within the recombinant polymer.

Commercially pure titanium is a biomaterial extensively used to make orthopedic and dental implants[174] because of its biocompatibility and suitable chemical (corrosion resistance) and mechanical properties (high tensile strength and elastic modulus).[175] However, titanium lacks the ability to rapidly osseointegrate, and bacterial colonization leads to biofilm formation, thus causing bone loss around the implant or peri-implantitis. In order to overcome these problems, it was proposed to incorporate antimicrobial properties into the implant. A solution to this problem involves coating the surfaces with antibacterial and biocompatible chitosan together with an osseoinductive recombinant elastin-like biopolymer (P-HAP) inspired by salival statherin.[176]

The successful attachment of chitosan and P-HAP to the titanium surface was achieved using a layer-by-layer (LbL) assembly technique, which provided chitosan/P-HAP bilayers on the titanium surface. This technique takes advantage of the different charge of the two polymers at physiological pH to establish ionic interactions between the two components of the bilayer, namely, HAP, which contains positively charged amine groups, and P-HAP, which contains negatively charged carboxyl groups.

The antibacterial activity of chitosan is believed to be due to its positively charged amines, which attract the negatively charged bacterial cell wall, thus disrupting cell dynamics and/or the cell membrane. In this regard, the recombinamer P-HAP contains the SN15 peptide (DDDEEKFLRRIGRFG), a domain present in salival statherin that is responsible for the protein's high affinity for HAP, the major component of enamel. The presence of this SN15 sequence can aid bone formation, and indeed, these polymers have previously shown an ability to induce biomineralization.[138] The LbL-modified surfaces were found to be effective against *Streptococcus gordonii*, a primary colonizer of tissues in the oral environment, showing a 50-fold decrease in the number of viable bacteria in comparison with uncoated titanium. DRIFTS spectra confirmed that LbL-modified surfaces showed biomimetic increased mineralization, with this mineralization increasing as the number of bilayers increased. These modified surfaces were found to be cytocompatible with mouse pre-osteoblast cells and had no significant effects on osteoblastic adhesion and differentiation, probably due to a detrimental decrease in the stiffness of the substrate.

Another approach to achieve biomineralization on the surface of implants, and thus improve their osseointegration, involves coating the implant surface with human salivary statherin-inspired genetically engineered recombinamers (ELRs, HSS) by covalent grafting. Thus, these biopolymers were tethered to nanorough titanium surfaces obtained by alkaline etching, and the ELRs were homogeneously distributed as thin layers that retained the original nanotopography of the substrate.[177] Subsequent mineralization using an enzyme-directed process resulted in a homogeneous layer of ACP on surfaces coated with ELR-HSS. The covalent immobilization of HSS-ELR via silane chemistry allowed control of the orientation of the bioactive molecules, thereby inducing and favoring spatial and temporal control of the growth of the CaP mineral layer. The nanotopographical features of the substrates had a positive influence on osteoprogenitor cell differentiation and bone growth,[178] as well as on bone-implant integration.[179,180] Indeed, both the disordered nanotopographical features and the CaP mineral layer contributed to stimulate differentiation of preosteoblastic cells (MC3T3-E1). An in vitro assay showed a significant increase in the number of adhered cells, which had a more spread morphology, and improved cell differentiation on nanorough surfaces with hybrid coatings of immobilized HSS-ELRs and a CaP mineral layer. The hybrid nanorough surfaces combined physical (disordered

nanotopography) and chemical (hybrid ELR/ACP) cues that enhanced differentiation of osteoprogenitor cells, thus showing potential for dental and orthopedic implant integration, especially for replacing and regenerating biological tissues.

8 | CONCLUSION

A comprehensive review of IDPs, such as ELRs, that are able to adapt assembled structures in response to intrinsic or extrinsic factors, has been provided in this manuscript. Almost half of the eukaryotic proteome contains IDPRs under physiological conditions that self-assemble to form ordered structures in order to maintain their biological activity. Many biological processes need ECM proteins enriched in disordered regions to carry out their functions, such as interaction with cell surface receptor and adhesion between cells and the matrix or focal adhesions. Herein, we have reviewed the different ways in which ELRs self-assemble depending on their amino acid sequence, for example, the ELR-based vesicles formed from diblock copolymers, which are functional structures useful for different biomedical applications. The recombinant nature of ELRs has allowed the development of numerous examples of constructs, such as modulable vesicles or micelles, by controlling both the structure of the ELRs and the conditions used. Taking advantage of their biocompatibility and effectiveness of drug encapsulationg, advanced nanodevices with potential uses for controlled drug delivery have been formed.

The combination of ELRs with those IDPRs that promote α-helical coil formation, including those mimicking collagen (CLPs) and those acting as zippers (ZELRs), has been shown to improve the properties of these biomaterials and allow their possible application in tissue engineering or controlled drug administration. In this sense, ZELRs have been used to develop new injectable hydrogels, and ELRs conjugated with CLPs have been used to design targeted drug-delivery devices.[98]

Multiblock co-recombinamers based on silk and elastin (SELRs) present a unique SA behavior controlled by the alternation of crystallizable and amorphous sequence motifs. The self-assembling behavior of these SELRs endows them with the appropriate characteristics to form stable physical hydrogels under physiological conditions. A further step has been taken by using them as biocompatible bioinks once a new, more complex smart material that allows the sequential gelling of a hydrogel had been developed.

Biomimetic scaffolds based on covalently cross-linked chemical ELR-based hydrogels form environments analogous to those in which cells are found in native tissues. New biocompatible ELR-based hydrogels have been reviewed, for example, those obtained using cytocompatible cross-linkers such as THPC, and the influence of hydrogel cross-link density and microstructure on cell response have been studied. Those hydrogels obtained using bio-orthogonal chemical techniques, such as SPAAC, have resulted in attractive biocompatible materials for biomedical applications because of their rapid gelation. Strong and self-adhesive hydrogels have been obtained from unstructured ELRs by covalent and reversible cross-linking, based on MCPs, thereby providing robust scaffolds for use in biomedical applications such as tissue engineering.

Biomineralization involves controlled deposition of calcium phosphate minerals into an organic matrix, and in this regard, hybrid nanocomposites with different morphologies have been obtained from porous hydrogels with different microstructures generated from ELRs carrying statherin-derived hydrophilic blocks (SNA15).

The final section has reviewed different ELR coatings of material surfaces using different techniques. Different bioactive ELRs have been deposited on substrates, grafting them using silanol chemistry or via cysteine-rich domains, as well as attaching them using LbL techniques. These coated surfaces have resulted in new systems for spatial control of cell adhesion, for BAI treatment or, in general, for enhancing tissue–material interactions. These new developments will be of great future interest in the fields of tissue engineering and regenerative medicine.

ACKNOWLEDGMENTS

The authors are grateful for funding from the Spanish Government (MAT2016-78903-R, RTI2018-096320-B-C22, PID2019-110709RB-100, and RED2018-102417-T), Junta de Castilla y León (VA317P18 and Infrared2018-UVA06), Interreg V España Portugal POCTEP (0624_2IQBIONEURO_6_E), and Centro en Red de Medicina Regenerativa y Terapia Celular de Castilla y León.

CONFLICT OF INTEREST

The authors declare no conflict of interest

AUTHOR CONTRIBUTIONS

M-S and D-JG have written the review and contributed to the conceptualization, literature search, drafting of the original sections, figure generation, and draft review. The graphical abstract was made with BioRender. JC-RC, V-R, and M-A contributed to the conceptualization, supervision, and sourcing funding for the team.

ORCID

Diana Juanes-Gusano https://orcid.org/0000-0001-5818-7371
Mercedes Santos https://orcid.org/0000-0003-2877-3235
José Carlos Rodríguez-Cabello https://orcid.org/0000-0002-3438-858X

REFERENCES

1. Whitesides GM, Grzybowski B. Self-assembly at all scales. *Science*. 2002;295(5564):2418-2421. https://doi.org/10.1126/science.1070821
2. Halley JD, Winkler DA. Consistent concepts of self-organization and self-assembly. *Complexity*. 2008;14(2):10-17. https://doi.org/10.1002/cplx.20235
3. Tantakitti F, Boekhoven J, Wang X, et al. Energy landscapes and functions of supramolecular systems. *Nat Mater*. 2016;15(4):469-476. https://doi.org/10.1038/nmat4538
4. da Silva RMP, van der Zwaag D, Albertazzi L, Lee SS, Meijer EW, Stupp SI. Super-resolution microscopy reveals structural diversity

in molecular exchange among peptide amphiphile nanofibres. *Nat Commun*. 2016;7(1):11561. https://doi.org/10.1038/ncomms11561
5. Aronsson C, Dånmark S, Zhou F, et al. Self-sorting heterodimeric coiled coil peptides with defined and tuneable self-assembly properties. *Sci Rep*. 2015;5(1):14063. https://doi.org/10.1038/srep14063
6. Discher BM, Won Y-Y, Ege DS, et al. Polymersomes: tough vesicles made from diblock copolymers. *Science*. 1999;284(5417):1143-1146. https://doi.org/10.1126/science.284.5417.1143
7. Ariga K, Hill JP, Lee MV, Vinu A, Charvet R, Acharya S. Challenges and breakthroughs in recent research on self-assembly. *Sci Technol Adv Mater*. 2008;9(1):14109. https://doi.org/10.1088/1468-6996/9/1/014109
8. Lee SS, Fyrner T, Chen F, et al. Sulfated glycopeptide nanostructures for multipotent protein activation. *Nat Nanotechnol*. 2017;12(8):821-829. https://doi.org/10.1038/nnano.2017.109
9. Okesola BO, Mata A. Multicomponent self-assembly as a tool to harness new properties from peptides and proteins in material design. *Chem Soc Rev*. 2018;47(10):3721-3736. https://doi.org/10.1039/c8cs00121a
10. Whitesides GM, Mathias JP, Seto CT. Molecular self-assembly and nanochemistry: a chemical strategy for the synthesis of nanostructures. *Science*. 1991;254(5036):1312-1319. https://doi.org/10.1126/science.1962191
11. Smithrud DB, Wyman TB, Diederich F. Enthalpically driven cyclophane-arene inclusion complexation: solvent-dependent calorimetric studies. *J Am Chem Soc*. 1991;113(14):5420-5426. https://doi.org/10.1021/ja00014a038
12. Huebsch N, Mooney DJ. Inspiration and application in the evolution of biomaterials. *Nature*. 2009;462(7272):426-432. https://doi.org/10.1038/nature08601
13. Boehr DD, Nussinov R, Wright PE. The role of dynamic conformational ensembles in biomolecular recognition. *Nat Chem Biol*. 2009;5(11):789-796. https://doi.org/10.1038/nchembio.232
14. Uversky VN. Intrinsically disordered proteins and their "mysterious" (meta)physics. *Front Phys*. 2019;7:10. https://doi.org/10.3389/fphy.2019.00010
15. Quintanilla-Sierra L, García-Arévalo C, Rodriguez-Cabello JC. Self-assembly in elastin-like recombinamers: a mechanism to mimic natural complexity. *Mater Today Bio*. 2019;2(1):100007. https://doi.org/10.1016/j.mtbio.2019.100007
16. Staby L, O'Shea C, Willemoës M, Theisen F, Kragelund BB, Skriver K. Eukaryotic transcription factors: paradigms of protein intrinsic disorder. *Biochem J*. 2017;474(15):2509-2532. https://doi.org/10.1042/BCJ20160631
17. van der Lee R, Buljan M, Lang B, et al. Classification of intrinsically disordered regions and proteins. *Chem Rev*. 2014;114(13):6589-6631. https://doi.org/10.1021/cr400525m
18. Dunker AK, Brown CJ, Lawson JD, Iakoucheva LM, Obradović Z. Intrinsic disorder and protein function. *Biochemistry*. 2002;41(21):6573-6582. https://doi.org/10.1021/bi012159
19. Uversky VN. Intrinsically disordered proteins and their (disordered) proteomes in neurodegenerative disorders. *Front Aging Neurosci*. 2015;7:18. https://doi.org/10.3389/fnagi.2015.00018
20. Uversky VN, Gillespie JR, Fink AL. Why are "natively unfolded" proteins unstructured under physiologic conditions? *Proteins Struct Funct Bioinforma*. 2000;41(3):415-427. https://doi.org/10.1002/1097-0134(20001115)41:3%3C415::AID-PROT130%3E3.0.CO;2-7
21. Acosta S, Quintanilla-Sierra L, Mbundi L, Reboto V, Rodríguez-Cabello JC. Elastin-like recombinamers: deconstructing and recapitulating the functionality of extracellular matrix proteins using recombinant protein polymers. *Adv Funct Mater*. 2020;30(44):1909050. https://doi.org/10.1002/adfm.201909050
22. Theillet F-X, Kalmar L, Tompa P, et al. The alphabet of intrinsic disorder. *Intrinsically Disord Proteins*. 2013;1(1):e24360. https://doi.org/10.4161/idp.24360
23. Habchi J, Tompa P, Longhi S, Uversky VN. Introducing protein intrinsic disorder. *Chem Rev*. 2014;114(13):6561-6588. https://doi.org/10.1021/cr400514h
24. Rath A, Davidson AR, Deber CM. The structure of "unstructured" regions in peptides and proteins: role of the polyproline ii helix in protein folding and recognition*. *Pept Sci*. 2005;80(2-3):179-185. https://doi.org/10.1002/bip.20227
25. Uversky VN. Natively unfolded proteins: a point where biology waits for physics. *Protein Sci*. 2002;11(4):739-756. https://doi.org/10.1110/ps.4210102
26. Babu MM. The contribution of intrinsically disordered regions to protein function, cellular complexity, and human disease. *Biochem Soc Trans*. 2016;44(5):1185-1200. https://doi.org/10.1042/BST20160172
27. Berlow RB, Dyson HJ, Wright PE. Functional advantages of dynamic protein disorder. *FEBS Lett*. 2015;589(19, Part A):2433-2440. https://doi.org/10.1016/j.febslet.2015.06.003
28. Nott TJ, Petsalaki E, Farber P, et al. Phase transition of a disordered nuage protein generates environmentally responsive membraneless organelles. *Mol Cell*. 2015;57(5):936-947. https://doi.org/10.1016/j.molcel.2015.01.013
29. Flock T, Weatheritt RJ, Latysheva NS, Babu MM. Controlling entropy to tune the functions of intrinsically disordered regions. *Curr Opin Struct Biol*. 2014;26:62-72. https://doi.org/10.1016/j.sbi.2014.05.007
30. Wright PE, Dyson HJ. Intrinsically disordered proteins in cellular signalling and regulation. *Nat Rev Mol Cell Biol*. 2015;16(1):18-29. https://doi.org/10.1038/nrm3920
31. Peysselon F, Xue B, Uversky VN, Ricard-Blum S. Intrinsic disorder of the extracellular matrix. *Mol Biosyst*. 2011;7(12):3353-3365. https://doi.org/10.1039/c1mb05316g
32. Dosztányi Z, Csizmok V, Tompa P, Simon I. IUPred: web server for the prediction of intrinsically unstructured regions of proteins based on estimated energy content. *Bioinformatics*. 2005;21(16):3433-3434. https://doi.org/10.1093/bioinformatics/bti541
33. Dosztányi Z, Csizmók V, Tompa P, Simon I. The pairwise energy content estimated from amino acid composition discriminates between folded and intrinsically unstructured proteins. *J Mol Biol*. 2005;347(4):827-839. https://doi.org/10.1016/j.jmb.2005.01.071
34. Romero P, Obradovic Z, Kissinger CR, et al. Thousands of proteins likely to have long disordered regions. *Pac Symp Biocomput*. 1998;437-448.
35. Banani SF, Lee HO, Hyman AA, Rosen MK. Biomolecular condensates: organizers of cellular biochemistry. *Nat Rev Mol Cell Biol*. 2017;18(5):285-298. https://doi.org/10.1038/nrm.2017.7
36. Crick SL, Ruff KM, Garai K, Frieden C, Pappu RV. Unmasking the roles of N- and C-terminal flanking sequences from exon 1 of huntingtin as modulators of polyglutamine aggregation. *Proc Natl Acad Sci*. 2013;110(50):20075-20080. https://doi.org/10.1073/pnas.1320626110
37. DeForte S, Uversky VN. Not an exception to the rule: the functional significance of intrinsically disordered protein regions in enzymes. *Mol Biosyst*. 2017;13(3):463-469. https://doi.org/10.1039/c6mb00741d
38. Uversky VN. Paradoxes and wonders of intrinsic disorder: complexity of simplicity. *Intrinsically Disord Proteins*. 2016;4(1):e1135015. https://doi.org/10.1080/21690707.2015.1135015
39. Uversky VN. Unusual biophysics of intrinsically disordered proteins. *Biochim Biophys Acta - Proteins Proteomics*. 2013;1834(5):932-951. https://doi.org/10.1016/j.bbapap.2012.12.008
40. Wise SG, Yeo GC, Hiob MA, et al. Tropoelastin: a versatile bioactive assembly module. *Acta Biomater*. 2014;10(4):1532-1541. https://doi.org/10.1016/j.actbio.2013.08.003

41. Yeo GC, Weiss AS. Soluble matrix protein is a potent modulator of mesenchymal stem cell performance. *Proc Natl Acad Sci*. 2019;116(6):2042-2051. https://doi.org/10.1073/pnas.1812951116
42. MacEwan SR, Chilkoti A. Elastin-like polypeptides: biomedical applications of tunable biopolymers. *Pept Sci*. 2010;94(1):60-77. https://doi.org/10.1002/bip.21327
43. Rosano GL, Ceccarelli EA. Recombinant protein expression in escherichia coli: advances and challenges. *Front Microbiol*. 2014;5:172. https://doi.org/10.3389/fmicb.2014.00172
44. Urry DW, Parker TM, Reid MC, Gowda DC. Biocompatibility of the bioelastic materials, poly (GVGVP) and its γ-irradiation cross-linked matrix: summary of generic biological test results. *J Bioact Compat Polym*. 1991;6(3):263-282. https://doi.org/10.1177/088391159100600306
45. Rodríguez-Cabello JC, Girotti A, Ribeiro A, Arias FJ. *Synthesis of Genetically Engineered Protein Polymers (Recombinamers) as an Example of Advanced Self-Assembled Smart Materials BT - Nanotechnology in Regenerative Medicine: Methods and Protocols*. In: Navarro M, Planell JA, eds. Totowa, NJ: Humana Press; 2012:17-38. https://doi.org/10.1007/978-1-61779-388-2_2
46. Li NK, Quiroz FG, Hall CK, Chilkoti A, Yingling YG. Molecular description of the LCST behavior of an elastin-like polypeptide. *Biomacromolecules*. 2014;15(10):3522-3530. https://doi.org/10.1021/bm500658w
47. Ruff KM, Roberts S, Chilkoti A, Pappu RV. Advances in understanding stimulus-responsive phase behavior of intrinsically disordered protein polymers. *J Mol Biol*. 2018;430(23):4619-4635. https://doi.org/10.1016/j.jmb.2018.06.031
48. Rodríguez-Cabello JC, Arias FJ, Rodrigo MA, Girotti A. Elastin-like polypeptides in drug delivery. *Adv Drug Deliv Rev*. 2016;97:85-100. https://doi.org/10.1016/j.addr.2015.12.007
49. Urry DW. Free energy transduction in polypeptides and proteins based on inverse temperature transitions. *Prog Biophys Mol Biol*. 1992;57(1):23-57. https://doi.org/10.1016/0079-6107(92)90003-O
50. Urry DW. Physical chemistry of biological free energy transduction as demonstrated by elastic protein-based polymers. *J Phys Chem B*. 1997;101(51):11007-11028. https://doi.org/10.1021/jp972167t
51. Rodríguez-Cabello JC, de Torre IG, Acosta S, Salinas S, Herrero M. In: Azevedo HS, da Silva RMPBT-SB, eds. *4 - Elastin-like Proteins: Molecular Design for Self-Assembling*. Woodhead Publishing Series in Biomaterials. Woodhead Publishing; 2018:49-78 https://doi.org/10.1016/B978-0-08-102015-9.00004-6
52. Pinedo-Martín G, Santos M, Testera AM, Alonso M, Rodríguez-Cabello JC. The effect of NaCl on the self-assembly of elastin-like block co-recombinamers: tuning the size of micelles and vesicles. *Polymer (Guildf)*. 2014;55(21):5314-5321. https://doi.org/10.1016/j.polymer.2014.08.053
53. Ferreira LA, Cole JT, Reichardt C, Holland NB, Uversky VN, Zaslavsky BY. Solvent properties of water in aqueous solutions of elastin-like polypeptide. *Int J Mol Sci*. 2015;16(6):13528-13547. https://doi.org/10.3390/ijms160613528
54. Ibáñez-Fonseca A, Flora T, Acosta S, Rodríguez-Cabello JC. Trends in the design and use of elastin-like recombinamers as biomaterials. *Matrix Biol*. 2019;84:111-126. https://doi.org/10.1016/j.matbio.2019.07.003
55. Rauscher S, Baud S, Miao M, Keeley FW, Pomès R. Proline and glycine control protein self-organization into elastomeric or amyloid fibrils. *Structure*. 2006;14(11):1667-1676. https://doi.org/10.1016/j.str.2006.09.008
56. Gronau G, Krishnaji ST, Kinahan ME, et al. A review of combined experimental and computational procedures for assessing biopolymer structure–process–property relationships. *Biomaterials*. 2012;33(33):8240-8255. https://doi.org/10.1016/j.biomaterials.2012.06.054
57. Muiznieks LD, Weiss AS, Keeley FW. Structural disorder and dynamics of elastin. *Biochem Cell Biol*. 2010;88(2):239-250. https://doi.org/10.1139/o09-161
58. Roberts S, Dzuricky M, Chilkoti A. Elastin-like polypeptides as models of intrinsically disordered proteins. *FEBS Lett*. 2015;589(19, Part A):2477-2486. https://doi.org/10.1016/j.febslet.2015.08.029
59. Wald T, Spoutil F, Osickova A, et al. Intrinsically disordered proteins drive enamel formation via an evolutionarily conserved self-assembly motif. *Proc Natl Acad Sci*. 2017;114(9):E1641-E1650. https://doi.org/10.1073/pnas.1615334114
60. Beniash E, Simmer JP, Margolis HC. Structural changes in amelogenin upon self-assembly and mineral interactions. *J Dent Res*. 2012;91(10):967-972. https://doi.org/10.1177/0022034512457371
61. Boskey AL, Villarreal-Ramirez E. Intrinsically disordered proteins and biomineralization. *Matrix Biol*. 2016;52–54:43-59. https://doi.org/10.1016/j.matbio.2016.01.007
62. Li Y, Rodriguez-Cabello JC, Aparicio C. Intrafibrillar mineralization of self-assembled elastin-like recombinamer fibrils. *ACS Appl Mater Interfaces*. 2017;9(7):5838-5846. https://doi.org/10.1021/acsami.6b15285
63. Roberts S, Harmon TS, Schaal JL, et al. Injectable tissue integrating networks from recombinant polypeptides with tunable order. *Nat Mater*. 2018;17(12):1154-1163. https://doi.org/10.1038/s41563-018-0182-6
64. Acosta S, Ye Z, Aparicio C, Alonso M, Rodríguez-Cabello JC. Dual self-assembled nanostructures from intrinsically disordered protein polymers with LCST behavior and antimicrobial peptides. *Biomacromolecules*. 2020;21(10):4043-4052. https://doi.org/10.1021/acs.biomac.0c00865
65. Acosta S, Ibañez-Fonseca A, Aparicio C, Rodríguez-Cabello JC. Antibiofilm coatings based on protein-engineered polymers and antimicrobial peptides for preventing implant-associated infections. *Biomater Sci*. 2020;8(10):2866-2877. https://doi.org/10.1039/d0bm00155d
66. Carlos Rodríguez-Cabello J, Reguera J, Girotti A, Alonso M, Testera AM. Developing functionality in elastin-like polymers by increasing their molecular complexity: the power of the genetic engineering approach. *Prog Polym Sci*. 2005;30(11):1119-1145. https://doi.org/10.1016/j.progpolymsci.2005.07.004
67. Akbarzadeh A, Rezaei-Sadabady R, Davaran S, et al. Liposome: classification, preparation, and applications. *Nanoscale Res Lett*. 2013;8(1):102. https://doi.org/10.1186/1556-276X-8-102
68. Tanner P, Baumann P, Enea R, Onaca O, Palivan C, Meier W. Polymeric vesicles: from drug carriers to nanoreactors and artificial organelles. *Acc Chem Res*. 2011;44(10):1039-1049. https://doi.org/10.1021/ar200036k
69. Brinkhuis RP, Rutjes FPJT, van Hest JCM. Polymeric vesicles in biomedical applications. *Polym Chem*. 2011;2(7):1449-1462. https://doi.org/10.1039/c1py00061f
70. Bleul R, Thiermann R, Maskos M. Techniques to control polymersome size. *Macromolecules*. 2015;48(20):7396-7409. https://doi.org/10.1021/acs.macromol.5b01500
71. Huber MC, Schreiber A, von Olshausen P, et al. Designer amphiphilic proteins as building blocks for the intracellular formation of organelle-like compartments. *Nat Mater*. 2015;14(1):125-132. https://doi.org/10.1038/nmat4118
72. Vargo KB, Parthasarathy R, Hammer DA. Self-assembly of tunable protein suprastructures from recombinant oleosin. *Proc Natl Acad Sci*. 2012;109(29):11657-11662. https://doi.org/10.1073/pnas.1205426109
73. Park WM, Champion JA. Thermally triggered self-assembly of folded proteins into vesicles. *J Am Chem Soc*. 2014;136(52):17906-17909. https://doi.org/10.1021/ja5090157

74. Vogele K, Frank T, Gasser L, et al. Towards synthetic cells using peptide-based reaction compartments. *Nat Commun*. 2018;9(1):3862. https://doi.org/10.1038/s41467-018-06379-8
75. Dreher MR, Simnick AJ, Fischer K, et al. Temperature triggered self-assembly of polypeptides into multivalent spherical micelles. *J Am Chem Soc*. 2008;130(2):687-694. https://doi.org/10.1021/ja0764862
76. Martín L, Castro E, Ribeiro A, Alonso M, Rodríguez-Cabello JC. Temperature-triggered self-assembly of elastin-like block co-recombinamers:the controlled formation of micelles and vesicles in an aqueous medium. *Biomacromolecules*. 2012;13(2):293-298. https://doi.org/10.1021/bm201436y
77. Vargo KB, Sood N, Moeller TD, Heiney PA, Hammer DA. Spherical micelles assembled from variants of recombinant oleosin. *Langmuir*. 2014;30(38):11292-11300. https://doi.org/10.1021/la502664e
78. Trabbic-Carlson K, Setton LA, Chilkoti A. Swelling and mechanical behaviors of chemically cross-linked hydrogels of elastin-like polypeptides. *Biomacromolecules*. 2003;4(3):572-580. https://doi.org/10.1021/bm025671z
79. Sallach RE, Wei M, Biswas N, et al. Micelle density regulated by a reversible switch of protein secondary structure. *J Am Chem Soc*. 2006;128(36):12014-12019. https://doi.org/10.1021/ja0638509
80. Ghoorchian A, Holland NB. Molecular architecture influences the thermally induced aggregation behavior of elastin-like polypeptides. *Biomacromolecules*. 2011;12(11):4022-4029. https://doi.org/10.1021/bm201031m
81. Hamley IW. Self-assembly of amphiphilic peptides. *Soft Matter*. 2011;7(9):4122-4138. https://doi.org/10.1039/c0sm01218a
82. Schreiber A, Stühn LG, Huber MC, Geissinger SE, Rao A, Schiller SM. Self-assembly toolbox of tailored supramolecular architectures based on an amphiphilic protein library. *Small*. 2019;15(30):1900163. https://doi.org/10.1002/smll.201900163
83. Schreiber A, Huber MC, Schiller SM. Prebiotic protocell model based on dynamic protein membranes accommodating anabolic reactions. *Langmuir*. 2019;35(29):9593-9610. https://doi.org/10.1021/acs.langmuir.9b00445
84. Hassouneh W, Zhulina EB, Chilkoti A, Rubinstein M. Elastin-like polypeptide diblock copolymers self-assemble into weak micelles. *Macromolecules*. 2015;48(12):4183-4195. https://doi.org/10.1021/acs.macromol.5b00431
85. Taniguchi S, Watanabe N, Nose T, Maeda I. Development of short and highly potent self-assembling elastin-derived pentapeptide repeats containing aromatic amino acid residues. *J Pept Sci*. 2016;22(1):36-42. https://doi.org/10.1002/psc.2837
86. Suyama K, Taniguchi S, Tatsubo D, Maeda I, Nose T. Dimerization effects on coacervation property of an elastin-derived synthetic peptide (FPGVG)5. *J Pept Sci*. 2016;22(4):236-243. https://doi.org/10.1002/psc.2876
87. Suyama K, Tatsubo D, Iwasaki W, et al. Enhancement of self-aggregation properties of linear elastin-derived short peptides by simple cyclization: strong self-aggregation properties of cyclo [FPGVG]n, consisting only of natural amino acids. *Biomacromolecules*. 2018;19(8):3201-3211. https://doi.org/10.1021/acs.biomac.8b00353
88. MacEwan SR, Weitzhandler I, Hoffmann I, Genzer J, Gradzielski M, Chilkoti A. Phase behavior and self-assembly of perfectly sequence-defined and monodisperse multiblock copolypeptides. *Biomacromolecules*. 2017;18(2):599-609. https://doi.org/10.1021/acs.biomac.6b01759
89. Martín L, Arias FJ, Alonso M, García-Arévalo C, Rodríguez-Cabello JC. Rapid micropatterning by temperature-triggered reversible gelation of a recombinant smart elastin-like tetrablock-copolymer. *Soft Matter*. 2010;6(6):1121-1124. https://doi.org/10.1039/b923684h
90. Coletta DJ, Ibáñez-Fonseca A, Missana LR, et al. Bone regeneration mediated by a bioactive and biodegradable extracellular matrix-like hydrogel based on elastin-like recombinamers. *Tissue Eng Part A*. 2017;23(23–24):1361-1371. https://doi.org/10.1089/ten.tea.2017.0047
91. Lombard C, Arzel L, Bouchu D, Wallach J, Saulnier J. Human leukocyte elastase hydrolysis of peptides derived from human elastin exon 24. *Biochimie*. 2006;88(12):1915-1921. https://doi.org/10.1016/j.biochi.2006.07.014
92. Luo T, Kiick KL. Collagen-like peptide bioconjugates. *Bioconjug Chem*. 2017;28(3):816-827. https://doi.org/10.1021/acs.bioconjchem.6b00673
93. Lupas AN, Gruber M. The structure of α-helical coiled coils. *Adv Protein Chem*. 2005;70:37-38. https://doi.org/10.1016/S0065-3233(05)70003-6
94. Wilson EO. The Encyclopedia of life. *Trends Ecol Evol*. 2003;18(2):77-80. https://doi.org/10.1016/S0169-5347(02)00040-X
95. Krylov D, Mikhailenko I, Vinson C. A thermodynamic scale for leucine zipper stability and dimerization specificity: E and g interhelical interactions. *EMBO J*. 1994;13(12):2849-2861. https://doi.org/10.1002/j.1460-2075.1994.tb06579.x
96. Crick FHC. The packing of α-helices: simple coiled-coils. *Acta Crystallogr*. 1953;6(8):689-697. https://doi.org/10.1107/s0365110x53001964
97. Jang Y, Choi WT, Heller WT, Ke Z, Wright ER, Champion JA. Engineering globular protein vesicles through tunable self-assembly of recombinant fusion proteins. *Small*. 2017;13(36):1700399. https://doi.org/10.1002/smll.201700399
98. Fernández-Colino A, Arias FJ, Alonso M, Rodríguez-Cabello JC. Amphiphilic elastin-like block co-recombinamers containing leucine zippers: cooperative interplay between both domains results in injectable and stable hydrogels. *Biomacromolecules*. 2015;16(10):3389-3398. https://doi.org/10.1021/acs.biomac.5b01103
99. Prhashanna A, Taylor PA, Qin J, Kiick KL, Jayaraman A. Effect of peptide sequence on the LCST-like transition of elastin-like peptides and elastin-like peptide–collagen-like peptide conjugates: simulations and experiments. *Biomacromolecules*. 2019;20(3):1178-1189. https://doi.org/10.1021/acs.biomac.8b01503
100. Luo T, Kiick KL. Noncovalent modulation of the inverse temperature transition and self-assembly of elastin-b-collagen-like peptide bioconjugates. *J Am Chem Soc*. 2015;137(49):15362-15365. https://doi.org/10.1021/jacs.5b09941
101. Luo T, David MA, Dunshee LC, et al. Thermoresponsive elastin-b-collagen-like peptide bioconjugate nanovesicles for targeted drug delivery to collagen-containing matrices. *Biomacromolecules*. 2017;18(8):2539-2551. https://doi.org/10.1021/acs.biomac.7b00686
102. Willems L, van Westerveld L, Roberts S, et al. Nature of amorphous hydrophilic block affects self-assembly of an artificial viral coat polypeptide. *Biomacromolecules*. 2019;20(10):3641-3647. https://doi.org/10.1021/acs.biomac.9b00512
103. Hardy JG, Römer LM, Scheibel TR. Polymeric materials based on silk proteins. *Polymer (Guildf)*. 2008;49(20):4309-4327. https://doi.org/10.1016/j.polymer.2008.08.006
104. Vepari C, Kaplan DL. Silk as a Biomaterial. *Prog Polym Sci*. 2007;32(8):991-1007. https://doi.org/10.1016/j.progpolymsci.2007.05.013
105. Fernández-Colino A, Arias FJ, Alonso M, Rodríguez-Cabello JC. Self-organized ECM-mimetic model based on an amphiphilic multiblock silk-elastin-like corecombinamer with a concomitant dual physical gelation process. *Biomacromolecules*. 2014;15(10):3781-3793. https://doi.org/10.1021/bm501051t
106. Ibáñez-Fonseca A, Orbanic D, Arias FJ, Alonso M, Zeugolis DI, Rodríguez-Cabello JC. Influence of the thermodynamic and kinetic control of self-assembly on the microstructure evolution of silk-

elastin-like recombinamer hydrogels. *Small*. 2020;16(28):2001244. https://doi.org/10.1002/smll.202001244
107. Willems L, Roberts S, Weitzhandler I, et al. Inducible fibril formation of silk–elastin diblocks. *ACS Omega*. 2019;4(5):9135-9143. https://doi.org/10.1021/acsomega.9b01025
108. Salinas-Fernández S, Santos M, Alonso M, Quintanilla L, Rodríguez-Cabello JC. Genetically engineered elastin-like recombinamers with sequence-based molecular stabilization as advanced bioinks for 3D bioprinting. *Appl Mater Today*. 2020;18:100500. https://doi.org/10.1016/j.apmt.2019.100500
109. Mbundi L, González-Pérez M, González-Pérez F, Juanes-Gusano D, Rodríguez-Cabello JC. Trends in the development of tailored elastin-like recombinamer–based porous biomaterials for soft and hard tissue applications. *Front Mater*. 2021;7:412. https://doi.org/10.3389/fmats.2020.601795
110. del Mercato LL, Maruccio G, Pompa PP, et al. Amyloid-like fibrils in elastin-related polypeptides: structural characterization and elastic properties. *Biomacromolecules*. 2008;9(3):796-803. https://doi.org/10.1021/bm7010104
111. Sharpe S, Simonetti K, Yau J, Walsh P. Solid-state NMR characterization of autofluorescent fibrils formed by the elastin-derived peptide GVGVAGVG. *Biomacromolecules*. 2011;12(5):1546-1555. https://doi.org/10.1021/bm101486s
112. Chung C, Lampe KJ, Heilshorn SC. Tetrakis (hydroxymethyl) phosphonium chloride as a covalent cross-linking agent for cell encapsulation within protein-based hydrogels. *Biomacromolecules*. 2012;13(12):3912-3916. https://doi.org/10.1021/bm3015279
113. Wang H, Paul A, Nguyen D, Enejder A, Heilshorn SC. Tunable control of hydrogel microstructure by kinetic competition between self-assembly and crosslinking of elastin-like proteins. *ACS Appl Mater Interfaces*. 2018;10(26):21808-21815. https://doi.org/10.1021/acsami.8b02461
114. Chung C, Pruitt BL, Heilshorn SC. Spontaneous cardiomyocyte differentiation of mouse embryoid bodies regulated by hydrogel crosslink density. *Biomater Sci*. 2013;1(10):1082-1090. https://doi.org/10.1039/C3BM60139K
115. Kambe Y, Tokushige T, Mahara A, Iwasaki Y, Yamaoka T. Cardiac differentiation of induced pluripotent stem cells on elastin-like protein-based hydrogels presenting a single-cell adhesion sequence. *Polym J*. 2019;51(1):97-105. https://doi.org/10.1038/s41428-018-0110-2
116. González de Torre I, Santos M, Quintanilla L, Testera A, Alonso M, Rodríguez Cabello JC. Elastin-like recombinamer catalyst-free click gels: characterization of poroelastic and intrinsic viscoelastic properties. *Acta Biomater*. 2014;10(6):2495-2505. https://doi.org/10.1016/j.actbio.2014.02.006
117. de Torre IG, Wolf F, Santos M, et al. Elastin-like recombinamer-covered stents: towards a fully biocompatible and non-thrombogenic device for cardiovascular diseases. *Acta Biomater*. 2015;12:146-155. https://doi.org/10.1016/j.actbio.2014.10.029
118. Contessotto P, Orbanić D, da Costa M, et al. Elastin-like recombinamers-based hydrogel modulates post-ischemic remodeling in a non-transmural myocardial infarction in sheep. *Sci Transl Med*. 2021;13(581):eaaz5380. https://doi.org/10.1126/scitranslmed.aaz5380
119. Madl CM, Katz LM, Heilshorn SC. Bio-orthogonally crosslinked, engineered protein hydrogels with tunable mechanics and biochemistry for cell encapsulation. *Adv Funct Mater*. 2016;26(21):3612-3620. https://doi.org/10.1002/adfm.201505329
120. Sun F, Zhang W-B, Mahdavi A, Arnold FH, Tirrell DA. Synthesis of bioactive protein hydrogels by genetically encoded spytag-spycatcher chemistry. *Proc Natl Acad Sci*. 2014;111(31):11269-11274. https://doi.org/10.1073/pnas.1401291111
121. Li L, Fierer JO, Rapoport TA, Howarth M. Structural analysis and optimization of the covalent association between spycatcher and a peptide tag. *J Mol Biol*. 2014;426(2):309-317. https://doi.org/10.1016/j.jmb.2013.10.021
122. Asai D, Xu D, Liu W, et al. Protein polymer hydrogels by in situ, rapid and reversible self-gelation. *Biomaterials*. 2012;33(21):5451-5458. https://doi.org/10.1016/j.biomaterials.2012.03.083
123. Gonzalez MA, Simon JR, Ghoorchian A, et al. Strong, tough, stretchable, and self-adhesive hydrogels from intrinsically unstructured proteins. *Adv Mater*. 2017;29(10):1604743. https://doi.org/10.1002/adma.201604743
124. Prescher JA, Bertozzi CR. Chemistry in living systems. *Nat Chem Biol*. 2005;1(1):13-21. https://doi.org/10.1038/nchembio0605-13
125. Sletten EM, Bertozzi CR. Bioorthogonal chemistry: fishing for selectivity in a sea of functionality. *Angew Chemie Int Ed*. 2009;48(38):6974-6998. https://doi.org/10.1002/anie.200900942
126. Rostovtsev VV, Green LG, Fokin VV, Sharpless KB. A stepwise huisgen cycloaddition process: copper(I)-catalyzed regioselective "ligation" of azides and terminal alkynes. *Angew Chem Int Ed Engl*. 2002;41(14):2596-2599. https://doi.org/10.1002/1521-3773(20020715)41:14%3C2596::AID-ANIE2596%3E3.0.CO;2-4
127. Tornøe CW, Christensen C, Meldal M. Peptidotriazoles on solid phase: [1,2,3]-triazoles by regiospecific copper(i)-catalyzed 1,3-dipolar cycloadditions of terminal alkynes to azides. *J Org Chem*. 2002;67(9):3057-3064. https://doi.org/10.1021/jo011148j
128. Baskin JM, Prescher JA, Laughlin ST, et al. Copper-free click chemistry for dynamic *in Vivo* imaging. *Proc Natl Acad Sci*. 2007;104(43):16793-16797. https://doi.org/10.1073/pnas.0707090104
129. Saxon E, Bertozzi CR. Cell surface engineering by a modified Staudinger reaction. *Science (80-.)*. 2000;287(5460):2007-2010. https://doi.org/10.1126/science.287.5460.2007
130. Devaraj NK, Weissleder R, Hilderbrand SA. Tetrazine-based cycloadditions: application to pretargeted live cell imaging. *Bioconjug Chem*. 2008;19(12):2297-2299. https://doi.org/10.1021/bc8004446
131. Jiang Y, Chen J, Deng C, Suuronen EJ, Zhong Z. Click hydrogels, microgels and nanogels: emerging platforms for drug delivery and tissue engineering. *Biomaterials*. 2014;35(18):4969-4985. https://doi.org/10.1016/j.biomaterials.2014.03.001
132. Addadi L, Weiner S. Control and design principles in biological mineralization. *Angew Chemie Int Ed English*. 1992;31(2):153-169. https://doi.org/10.1002/anie.199201531
133. Fang P-A, Conway JF, Margolis HC, Simmer JP, Beniash E. Hierarchical Self-Assembly of Amelogenin and the Regulation of Biomineralization at the Nanoscale. *Proc Natl Acad Sci*. 2011;108(34):14097-14102. https://doi.org/10.1073/pnas.1106228108
134. Landis WJ, Hodgens KJ, Arena J, Song MJ, McEwen BF. Structural relations between collagen and mineral in bone as determined by high voltage electron microscopic tomography. *Microsc Res Tech*. 1996;33(2):192-202. https://doi.org/10.1002/(SICI)1097-0029(19960201)33:2%3C192::AID-JEMT9%3E3.0.CO;2-V
135. Olszta MJ, Cheng X, Jee SS, et al. Bone structure and formation: a new perspective. *Mater Sci Eng R Reports*. 2007;58(3):77-116. https://doi.org/10.1016/j.mser.2007.05.001
136. Cantaert B, Beniash E, Meldrum FC. Nanoscale confinement controls the crystallization of calcium phosphate: relevance to bone formation. *Chem – A Eur J*. 2013;19(44):14918-14924. https://doi.org/10.1002/chem.201302835
137. Shoulders MD, Raines RT. Collagen structure and stability. *Annu Rev Biochem*. 2009;78(1):929-958. https://doi.org/10.1146/annurev.biochem.77.032207.120833
138. Li Y, Chen X, Fok A, Rodriguez-Cabello JC, Aparicio C. Biomimetic mineralization of recombinamer-based hydrogels toward controlled

morphologies and high mineral density. *ACS Appl Mater Interfaces*. 2015;7(46):25784-25792. https://doi.org/10.1021/acsami.5b07628
139. Nudelman F, Pieterse K, George A, et al. The role of collagen in bone apatite formation in the presence of hydroxyapatite nucleation inhibitors. *Nat Mater*. 2010;9(12):1004-1009. https://doi.org/10.1038/nmat2875
140. Elsharkawy S, Al-Jawad M, Pantano MF, et al. Protein disorder–order interplay to guide the growth of hierarchical mineralized structures. *Nat Commun*. 2018;9(1):2145. https://doi.org/10.1038/s41467-018-04319-0
141. Shah S, Kosoric J, Hector MP, Anderson P. An in vitro scanning microradiography study of the reduction in hydroxyapatite demineralization rate by statherin-like peptides as a function of increasing N-terminal length. *Eur J Oral Sci*. 2011;119(s1):13-18. https://doi.org/10.1111/j.1600-0722.2011.00899.x
142. Tejeda-Montes E, Klymov A, Nejadnik MR, et al. Mineralization and bone regeneration using a bioactive elastin-like recombinamer membrane. *Biomaterials*. 2014;35(29):8339-8347. https://doi.org/10.1016/j.biomaterials.2014.05.095
143. Ho CY, Shanahan CM. Medial arterial calcification. *Arterioscler Thromb Vasc Biol*. 2016;36(8):1475-1482. https://doi.org/10.1161/ATVBAHA.116.306717
144. Amann K. Media calcification and intima calcification are distinct entities in chronic kidney disease. *Clin J Am Soc Nephrol*. 2008;3(6):1599-1605. https://doi.org/10.2215/CJN.02120508
145. Gourgas O, Cole GB, Muiznieks LD, Sharpe S, Cerruti M. Effect of the ionic concentration of simulated body fluid on the minerals formed on cross-linked elastin-like polypeptide membranes. *Langmuir*. 2019;35(47):15364-15375. https://doi.org/10.1021/acs.langmuir.9b02542
146. Ophélie G, Juliana M, Peng Z, Monzur M, Marta C. Multidisciplinary approach to understand medial arterial calcification. *Arterioscler Thromb Vasc Biol*. 2018;38(2):363-372. https://doi.org/10.1161/ATVBAHA.117.309808
147. Jiang X, Bruzewicz DA, Wong AP, Piel M, Whitesides GM. Directing cell migration with asymmetric micropatterns. *Proc Natl Acad Sci U S A*. 2005;102(4):975-978. https://doi.org/10.1073/pnas.0408954102
148. Patrito N, McCague C, Norton PR, Petersen NO. Spatially controlled cell adhesion via micropatterned surface modification of poly (dimethylsiloxane). *Langmuir*. 2007;23(2):715-719. https://doi.org/10.1021/la062007l
149. Chua P-H, Neoh K-G, Kang E-T, Wang W. Surface functionalization of titanium with hyaluronic acid/chitosan polyelectrolyte multilayers and RGD for promoting osteoblast functions and inhibiting bacterial adhesion. *Biomaterials*. 2008;29(10):1412-1421. https://doi.org/10.1016/j.biomaterials.2007.12.019
150. Pham VTH, Bhadra CM, Truong VK, Crawford RJ, Ivanova EP. *Designing Antibacterial Surfaces for Biomedical Implants BT - Antibacterial Surfaces*. In: Ivanova E, Crawford R, eds. Springer International Publishing: Cham; 2015:89-111. https://doi.org/10.1007/978-3-319-18594-1_6
151. Cloutier M, Mantovani D, Rosei F. Antibacterial coatings: challenges, perspectives, and opportunities. *Trends Biotechnol*. 2015;33(11):637-652. https://doi.org/10.1016/j.tibtech.2015.09.002
152. Li L, Mo C-K, Chilkoti A, Lopez GP, Carroll NJ. Creating cellular patterns using genetically engineered. *Gold- and Cell-Binding Polypeptides. Biointerphases*. 2016;11(2):21009. https://doi.org/10.1116/1.4952452
153. Flora T, de Torre IG, Quintanilla L, Alonso M, Rodríguez-Cabello JC. Spatial control and cell adhesion selectivity on model gold surfaces grafted with elastin-like recombinamers. *Eur Polym J*. 2018;106:19-29. https://doi.org/10.1016/j.eurpolymj.2018.06.026
154. Lu Y, Chen SC. Micro and nano-fabrication of biodegradable polymers for drug delivery. *Adv Drug Deliv Rev*. 2004;56(11):1621-1633. https://doi.org/10.1016/j.addr.2004.05.002
155. Salvagni E, Berguig G, Engel E, et al. A bioactive elastin-like recombinamer reduces unspecific protein adsorption and enhances cell response on titanium surfaces. *Colloids Surfaces B Biointerfaces*. 2014;114:225-233. https://doi.org/10.1016/j.colsurfb.2013.10.008
156. Kasemo B. Biological Surface Science. *Surf Sci*. 2002;500(1):656-677. https://doi.org/10.1016/S0039-6028(01)01809-X
157. Albrektsson T, Jacobsson M. Bone-metal interface in osseointegration. *J Prosthet Dent*. 1987;57(5):597-607. https://doi.org/10.1016/0022-3913(87)90344-1
158. Castner DG, Ratner BD. Biomedical surface science: foundations to frontiers. *Surf Sci*. 2002;500(1):28-60. https://doi.org/10.1016/S0039-6028(01)01587-4
159. Bagheri M, Beyermann M, Dathe M. Immobilization reduces the activity of surface-bound cationic antimicrobial peptides with no influence upon the activity spectrum. *Antimicrob Agents Chemother*. 2009;53(3):1132-1141. https://doi.org/10.1128/AAC.01254-08
160. Zaborowska M, Welch K, Brånemark R, et al. Bacteria-material surface interactions: methodological development for the assessment of implant surface induced antibacterial effects. *J Biomed Mater Res Part B Appl Biomater*. 2015;103(1):179-187. https://doi.org/10.1002/jbm.b.33179
161. Bazaka K, Jacob MV, Crawford RJ, Ivanova EP. Efficient surface modification of biomaterial to prevent biofilm formation and the attachment of microorganisms. *Appl Microbiol Biotechnol*. 2012;95(2):299-311. https://doi.org/10.1007/s00253-012-4144-7
162. Campoccia D, Montanaro L, Arciola CR. The significance of infection related to orthopedic devices and issues of antibiotic resistance. *Biomaterials*. 2006;27(11):2331-2339. https://doi.org/10.1016/j.biomaterials.2005.11.044
163. Ye Z, Zhu X, Acosta S, Kumar D, Sang T, Aparicio C. Self-assembly dynamics and antimicrobial activity of All l- and d-amino acid enantiomers of a designer peptide. *Nanoscale*. 2019;11(1):266-275. https://doi.org/10.1039/c8nr07334a
164. Atefyekta S, Pihl M, Lindsay C, Heilshorn SC, Andersson M. Antibiofilm elastin-like polypeptide coatings: functionality, stability, and selectivity. *Acta Biomater*. 2019;83:245-256. https://doi.org/10.1016/j.actbio.2018.10.039
165. Haynie SL, Crum GA, Doele BA. Antimicrobial activities of amphiphilic peptides covalently bonded to a water-insoluble resin. *Antimicrob Agents Chemother*. 1995;39(2):301-307. https://doi.org/10.1128/AAC.39.2.301
166. Willcox MDP, Hume EBH, Aliwarga Y, Kumar N, Cole N. A novel cationic-peptide coating for the prevention of microbial colonization on contact lenses. *J Appl Microbiol*. 2008;105(6):1817-1825. https://doi.org/10.1111/j.1365-2672.2008.03942.x
167. Acosta S, Quintanilla L, Alonso M, Aparicio C, Rodríguez-Cabello JC. Recombinant AMP/polypeptide self-assembled monolayers with synergistic antimicrobial properties for bacterial strains of medical relevance. *ACS Biomater Sci Eng*. 2019;5(9):4708-4716. https://doi.org/10.1021/acsbiomaterials.9b00247
168. Andersson L, Blomberg L, Flegel M, Lepsa L, Nilsson B, Verlander M. Large-scale synthesis of peptides. *Pept Sci*. 2000;55(3):227-250. https://doi.org/10.1002/1097-0282(2000)55:3%3C227::AID-BIP50%3E3.0.CO;2-7
169. Wu WY, Mee C, Califano F, Banki R, Wood DW. Recombinant protein purification by self-cleaving aggregation tag. *Nat Protoc*. 2006;1(5):2257-2262. https://doi.org/10.1038/nprot.2006.314
170. Hassouneh W, Christensen T, Chilkoti A. Elastin-like polypeptides as a purification tag for recombinant proteins. *Curr Protoc Protein Sci*. 2010;61(1):6.11.1-6.11.16. https://doi.org/10.1002/0471140864.ps0611s61

171. Wadhwani P, Heidenreich N, Podeyn B, Bürck J, Ulrich AS. Antibiotic gold: tethering of antimicrobial peptides to gold nanoparticles maintains conformational flexibility of peptides and improves trypsin susceptibility. *Biomater Sci*. 2017;5(4):817-827. https://doi.org/10.1039/c7bm00069c
172. Salwiczek M, Qu Y, Gardiner J, et al. Emerging rules for effective antimicrobial coatings. *Trends Biotechnol*. 2014;32(2):82-90. https://doi.org/10.1016/j.tibtech.2013.09.008
173. Wisdom EC, Zhou Y, Chen C, Tamerler C, Snead ML. Mitigation of peri-implantitis by rational design of bifunctional peptides with antimicrobial properties. *ACS Biomater Sci Eng*. 2020;6(5):2682-2695. https://doi.org/10.1021/acsbiomaterials.9b01213
174. Norowski PA Jr, Bumgardner JD. Biomaterial and antibiotic strategies for peri-implantitis: a review. *J Biomed Mater Res Part B Appl Biomater*. 2009;88B(2):530-543. https://doi.org/10.1002/jbm.b.31152
175. Aparicio C, Javier Gil F, Fonseca C, Barbosa M, Planell JA. Corrosion behaviour of commercially pure titanium shot blasted with different materials and sizes of shot particles for dental implant applications. *Biomaterials*. 2003;24(2):263-273. https://doi.org/10.1016/S0142-9612(02)00314-9
176. Govindharajulu JP, Chen X, Li Y, Rodriguez-Cabello JC, Battacharya M, Aparicio C. Chitosan-recombinamer layer-by-layer coatings for multifunctional implants. *Int J Mol Sci*. 2017;18(2):369. https://doi.org/10.3390/ijms18020369
177. Li Y, Chen X, Ribeiro AJ, et al. Hybrid nanotopographical surfaces obtained by biomimetic mineralization of statherin-inspired elastin-like recombinamers. *Adv Healthc Mater*. 2014;3(10):1638-1647. https://doi.org/10.1002/adhm.201400015
178. Dalby MJ, Gadegaard N, Oreffo ROC. Harnessing nanotopography and integrin–matrix interactions to influence stem cell fate. *Nat Mater*. 2014;13(6):558-569. https://doi.org/10.1038/nmat3980
179. Prodanov L, Lamers E, Domanski M, Luttge R, Jansen JA, Walboomers XF. The effect of nanometric surface texture on bone contact to titanium implants in rabbit tibia. *Biomaterials*. 2013;34(12):2920-2927. https://doi.org/10.1016/j.biomaterials.2013.01.027
180. Lavenus S, Trichet V, le Chevalier S, Hoornaert A, Louarn G, Layrolle P. Cell differentiation and osseointegration influenced by nanoscale anodized titanium surfaces. *Nanomedicine*. 2012;7(7):967-980. https://doi.org/10.2217/nnm.11.181

AUTHOR BIOGRAPHIES

Diana Juanes-Gusano is undertaking her PhD in the Bioforge lab at the University of Valladolid. She obtained an MS in Chemistry with a specialty in professional profile from the University of Salamanca in 2015 and a BA in Chemistry from the same University in 2014. Her research is on designing biomaterials based on elastin-like recombinamers for tissue regeneration. Her main research interest is biofabrication of smart materials for biomedical applications exploring the clinical efficacy.

Mercedes Santos is a Professor of Chemistry at the University of Valladolid. She is a member of Bioforge, an interdisciplinar research group dedicated to the development of elastin-like biopolymers as a base for advanced biomaterials with potential use in regenerative medicine, and cofounder of the Company Technical Proteins Nanobiotechnology SL. Her interests include synthesis and biofunctionalization of elastin-like recombinant polymers so as their application in different fields as tissue engineering, controlled drug delivery, and nanomedicine.

Virginia Reboto is a Professor of Chemistry at the University of Valladolid. She is a member of Bioforge from their formation, an interdisciplinar research group dedicated to the development of elastin-like biopolymers as a base for advanced biomaterials with potential use in regenerative medicine. Her interests include the bioproduction of elastin-like recombinant polymers so as their smart nature.

Matilde Alonso is a Professor of Chemistry at the University of Valladolid. She is member of the Bioforge Lab, from their formation, founded in 1996 and cofounder of the company Technical Proteins Nanobiotechnology SL. She is interested in the development of elastin-type materials with different functionalities that improve their behavior in application systems in regenerative medicine and drug delivery.

José Carlos Rodríguez-Cabello is a Professor of Physics at the University of Valladolid. He is the Chief Executive Officer and cofounder of the company Technical Proteins Nanobiotechnology SL. He is the director of the Bioforge Lab, a research group founded in 1996 and devoted to the development of elastin-like materials in a pioneering effort for the use of genetic engineering and other biotechnologies for the creation of advanced materials. His interests range from studying basic knowledge on self-organization and the interplay between order and disorder in protein-like systems to applications of those materials in fields such as regenerative medicine, nanomedicine, and nanotechnology. Complexity and multi(bio)functionality are the characteristics of the systems developed by his group.

How to cite this article: Juanes-Gusano D, Santos M, Reboto V, Alonso M, Rodríguez-Cabello JC. Self-assembling systems comprising intrinsically disordered protein polymers like elastin-like recombinamers. *J Pep Sci*. 2022;28(1):e3362. doi:10.1002/psc.3362